energies

MDPI

Review

Leakage Current Measurements of Surge Arresters

Marek Olesz, Leszek S. Litzbarski and Grzegorz Redlarski *

Department of Electrical and Control Engineering, Gdańsk University of Technology, Narutowicza 11/12, 80-233 Gdańsk, Poland; marek.olesz@pg.edu.pl (M.O.); leszek.litzbarski@pg.edu.pl (L.S.L.)
* Correspondence: grzegorz.redlarski@pg.edu.pl

Abstract: The paper presents the methods of assessing the technical condition of varistor surge arresters used in laboratory tests and in operation—performed without disconnecting the arresters from the network. The analysis of the diagnostic methods was supplemented with the results of the measurements of the leakage current of arresters coming directly from their production and used in the power industry. Among the available methods of evaluating the technical condition of arresters, mainly indicator solutions (temperature and operation counter) and the measurement of the selected parameters of the leakage current are used. In the latter, the method of determining the resistive component of the leakage current, determined on the basis of the analysis of the voltage and current waveforms, or only the arrester current, has become widespread. In this type of measurement, current clamps are used in the operation, and additionally, in voltage measurements, voltage transformers are used, where you have to take into account the fundamental, additional sources of errors discussed in the article. These errors and the dispersion resulting from the production technology may fundamentally hinder the proper assessment of the technical condition; hence, it is so important to properly recognize the listed basic sources of measurement uncertainty. In addition, the analysis should take into account three factors related to external conditions: temperature, the voltage applied to the arrester, and the content of higher harmonics in the supply voltage, for which appropriate methods have been provided to determine the active component of the leakage current for reference conditions. This article presents the results of the measurements of the leakage currents of surge arresters measured with various methods.

Keywords: surge arresters; varistors; diagnostic; leakage current; the real part of the leakage current

Citation: Olesz, M.; Litzbarski, L.S.; Redlarski, G. Leakage Current Measurements of Surge Arresters. *Energies* **2023**, *16*, 6480. https://doi.org/10.3390/en16186480

Academic Editor: Adel Mellit

Received: 28 June 2023
Revised: 14 August 2023
Accepted: 4 September 2023
Published: 7 September 2023

1. Introduction

High voltage surge arresters have an important role in power systems, especially in protecting the insulation of power lines and transformers against lightning and switching overvoltages. However, in order to ensure an appropriate protection, it is necessary to cascade them with MV and LV ones, which is commonly known as a protection in depth. Their appropriate selection makes it possible to obtain proper insulation coordination between the electrical strength of the protected insulation and the level of protection clearly defined by the protective characteristics of surge arresters. A periodical inspection of the technical condition of the arrester allows the maintenance of the insulation coordination margin to be controlled and thus ensures the correct operation of the transformer in the conditions of voltage exposure. Information on the condition of surge arresters—similarly to other elements of the energy system—should be obtained already at the level of acceptance measurements so as to determine the operationally acceptable reference levels of the arrester's quality indicators and the planned method of the earlier liquidation of elements characterized by poor technical condition. This approach allows for higher operational reliability of the energy system, in which emergency shutdowns of the network are undesirable phenomena due to the problems of maintaining the continuity of electricity supply to consumers.

The basic elements of the arrester are varistors made on the basis of zinc oxide ZnO (semiconductor) with many appropriate admixtures (mainly bismuth), which, as a consequence of the multi-phase structure, are characterized by non-linear voltage–current characteristics.

For the voltage–current characteristics of the varistor in the initial range, it is observed at voltages forcing the flow of small currents (e.g., up to 1 mA (Figure 1, point (I1, U1)), with the resistance value of the varistor in the order of gigaohms. On the other hand, for a small change in the voltage, U, in the area of the so-called breakdown (Figure 1, point (I2, U2)), the current, I, reaches values of the order of kiloamperes, which is usually described by the power relationship (1):

$$I = kU^{\alpha} \quad (1)$$

where k is a constant depending on the geometry of the varistor and its synthesis process, and α is a nonlinearity coefficient defined as α = [d (lnI)/d (ln) V] and usually lies in the range 30–100 [1].

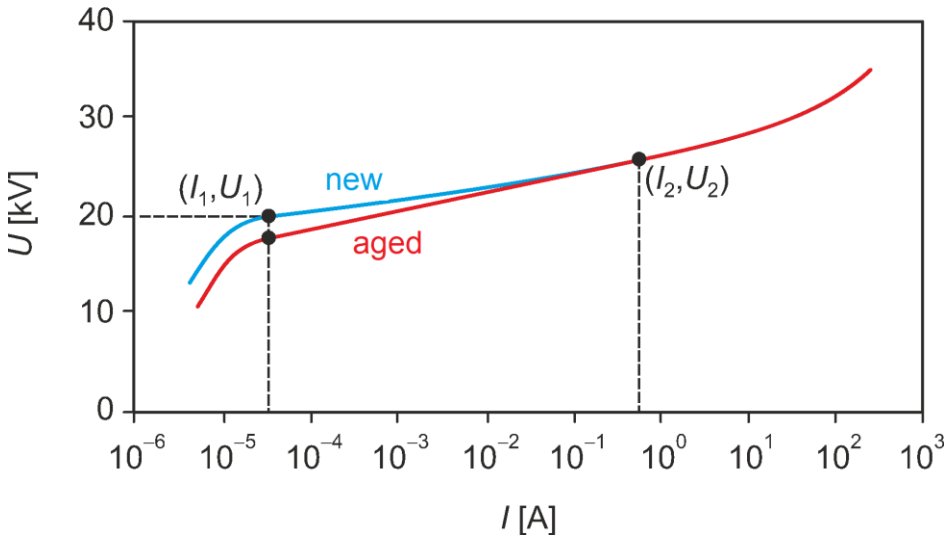

Figure 1. U(I) characteristics of a new and aged surge arrester.

At higher voltages, due to the reduction in the barriers between the grains, the current conduction character of the varistor is typically resistive, with a resistance of a few ohms [2].

Laboratory tests show that in ZnO ceramics, in the case of high-frequency waveforms of the order of 1 MHz, typical for lightning overvoltages, there is a maximum dielectric loss factor. An increase in the temperature of the arrester strongly favors an increase in its conductive properties. An increase in the leakage and polarization currents is then observed. In addition, aging with current surges causes a shift to the right of the voltage–current characteristics, which is physically associated with a change in the grain size distribution in the varistor volume—especially as a result of negative polarity surges. This phenomenon is related to the influence of temperature on the conduction mechanisms, especially in smaller varistors (e.g., low voltage), where relatively small exposures, due to weaker absorption of current surges, can cause strong heating of the varistor and change its U(I) characteristic, which shifts to the right towards larger currents [2–4].

There are a few parameters used commonly to describe the electrical properties of surge arresters. One of them is residual voltage (U_{res}), which can be defined as a crest value of the voltage measured between the terminals of an arrester due to the discharge current having a current waveshape of 8 µs/20 µs. Another useful parameter is the leakage current (I_L), which stands for a current passing through the arrester during the tests at the maximum continuous operating AC voltage (U_c) [3].

The electrical properties of ZnO-based varistors originate from the microstructure of these multicomponent ceramics. A typical chemical composition of these materials consists

of ZnO (>95%), Bi_2O_3 (1%), Sb_2O_3 (1%) and trace amounts of other additives, which have a large impact on the electrical properties of varistors [5]. Metal oxide surge arresters have a typical ceramic microstructure and consist of semiconducting ZnO grains separated by pores and grain boundary layers, which are formed predominantly by Bi_2O_3 [6]. The dimensions of ZnO grains can be controlled by the addition of Sb_2O_3, which crystallize in a spinel-like structure [7]. Furthermore, in order to improve the sintering process, NiO is usually used [8]. Other dopants modify the electrical properties of varistors, e.g., the upturn characteristic may be reduced by Co_2O_3 [9] and MnO [10], whilst Cr_2O_3 [11,12] promotes the nonlinearity of I(U) dependence. Moreover, Cr_2O_3 was found to lower the leakage current value [13]. Experiments were also performed with the use of other additives, e.g., alkali oxides [14] or rare earth oxides [15]. The parameters of the varistors depends not only to a chemical composition but also on the synthesis process. The value of U_{res} strongly depends on the size of the ZnO grains, which can be changed via the modification of the sintering time or temperature [16]. The high heating rate also increases the breakdown voltage; however, it may have a negative influence on the leakage current and the nonlinearity coefficient [17]. Moreover, the α coefficient is sensitive to the high sintering temperature, which is probably a result of the volatilization of Bi_2O_3 [18]. The dielectric losses are another parameter altered by the sintering temperature changes [19].

Regardless of the numerous advantages of ZnO-based varistors, the impact of overvoltage often causes varying failures of these devices [20]. The repeated lightning strokes lead to the degradation of the structure of metal oxide surge arresters and, in consequence, deteriorate their electrical parameters [21]. For this reason, it is necessary to assess the technical condition of these devices. The aging process of varistors causes an essential increase in the leakage current (especially its effective component), which is widely used in diagnostic processes. In this article, we described the most important methods of the leakage current investigations and technical issues affecting the quality of these measurements.

2. Methods of Diagnosing Surge Arresters

At the level of LV and MV grids, the commercial power industry usually operates the surge arresters until they fail, and any checks usually force the voltage to be switched off, the surge arrester disconnected from the grid system, measurements carried out using external voltage sources, and a decision to replace or reconnect the apparatus to the grid. From the point of view of lightning and surge protection, it is periodically checked according to the internal operating instructions: in the scope of visual inspection—condition of insulators (cracks, scratches, traces of surface discharges), corrosion condition of fittings and connecting wires, damage or too high mechanical stress, number of surge arresters, value of leakage current, condition of earthing connections—condition of the conductor, continuity, corrosion, protective coatings. The result is an inspection card on which the condition of the device is entered: good, medium (within the scheduled date) and bad (immediate repair).

As part of a specialist or ad hoc review, specific lists of measurement activities can be proposed. This applies in particular to the area of power substations in the HV area, where power utilities have introduced their own inspection procedures consisting of testing surge arresters disconnected from the network or assessed online. Then, in order to assess surge arresters, the permissible levels of leakage current or reference voltage are given. For example, the manufacturer of the Tridelta arrester type SBK-II 96/10.2 expects a reference voltage level in the range of 101.6–106.3 kV when inducing a leakage current of a maximum value of 5 mA. In HV grid systems, the shutdown of the voltage is usually limited, and in this case, the activities are usually in the form of continuous measurements monitoring the technical condition of the surge arresters, especially in places providing overvoltage protection for distribution systems at the transformer/switching station (T/S_S).

Recommendations for the diagnostics of MV and HV spark-free surge arresters are provided in Appendix D to the standard [2], which contains guidelines for their use and selection. The standard applies to surge arresters that will be operated in three-phase

systems with a nominal voltage above 1 kV. The supplement is a review of the methods widely used in the power engineering of the facility, unfortunately based on a literature review from the years up to and including 1993, and proposes the use of simple technical solutions consisting of the introduction of:

- Damage indicators that do not disconnect the arrester from the network but only indicate the technical condition by indicating the amplitude and time of current flow or the temperature of the varistors;
- Devices signaling the state of the partial or complete destruction of a varistor element (e.g., disconnectors);
- Special devices measuring the number and/or amplitude of current and/or voltage surges;
- Series spark gaps in the solutions requiring disconnection from the network or remaining in the network system;
- Temperature analyzers;
- Measurements of harmonic leakage current or active power losses.

Indicator devices are a component of a complete arrester or its additional element connected in series and are divided into fault indicators, disconnectors and operation counters. The damage of an indicator, in the case of exceeding the current amplitude or the duration of a certain critical current value, only indicates this fact without the automatic disconnection of the arrester from the network. The disconnector, in turn, is designed to isolate the arrester from the network system at the time of its failure. Typically, an explosive element (solutions for MV) is used for this purpose, triggered by the flow of a short-circuit current of a certain amplitude and duration. The disadvantage of the applied solution is the fact that after the arrester is disconnected, there is no overvoltage protection in the power network section until it is replaced.

Another way to determine the degree of degradation of the surge arrester is to use a trip counter triggered by a discharge current exceeding a certain amplitude. In the case of multiple discharges with times between discharges of less than 50 ms, due to the design of the counting system, not all discharges may be counted. In some designs, a sufficiently long follow-up current flow is required for the meter to work, which may cause difficulties in counting short discharge currents.

An interesting method of analyzing the state of the surge arrester is to use a thermal imaging camera. The intensive heating of the varistor structure causes a local increase in the temperature of the insulation of the housing, indicating problems with the varistor or water penetration into the housing and a local increase in surface currents in the varistor stack.

However, from the methods proposed by the standard [2], the methods based on the determination of the leakage current and its resistive component gained special importance in the online diagnostics of HV arresters and in the off-line diagnostics of MV and LV arresters. The standard specifies the level of the capacitive component in the range of 0.2 to 3 mA, depending on the capacitance of the arrester, which is typically $60 \div 150$ pF per kV of the rated voltage, referred to as an area of 1 cm^2 of the varistor element. The diagram given in the standard gives a typical U/U_r characteristic, indicating a leakage current of about 1 mA at a voltage of 0.6 U_r. Doubling the active component usually causes a slight increase of approx. 10% of the leakage current, which means that the main diagnostic effort goes towards the development of methods analyzing the active component of the leakage current, in which the third harmonic of this current has a significant share of the active current (from 10 to 40%).

In most cases, in the power industry, there are methods that ensure the constant monitoring of the leakage current of limiters, unfortunately in the presence of frequent external disturbances. The standard for calculating the active component proposes various methods of leakage current analysis (e.g., a method of using a voltage signal as a reference, a method of compensating the capacitive component using a voltage signal, a method of compensation without using a voltage signal, a method of compensation using the analysis

of currents in three phases and a harmonic analysis using the following methods: harmonic, third harmonic with harmonic compensation in the mains voltage and first-order harmonic analysis). Table 5 in [2] indicates that in professional practice, the methods of the analysis of the harmonics of the leakage current are generally used, the origins of which date back to the 1980s.

An undoubted advantage of the harmonic analysis method is the ability to measure the state of the arrester without disconnecting it from the network. Due to the significant error resulting from the content of the third harmonic in the supply voltage, even within the range of 100–350%, in practice, the method of third harmonic analysis with compensation with the signal related to the third harmonic of the limiter's capacitive current has become the most popular. In practice, the method of measuring the leakage current based on the determination of the active component or the power of losses isolated on the arrester is most often used. Both the measurements taken with the surge arrester connected to the network (operational) and disconnected from the network (laboratory with DC or AC voltage) are used. In order to enable the measurement of the leakage current, a special insulated earthing clamp is installed between the arrester and the earthing, to which a measuring device is connected periodically (periodic diagnostics) or permanently (monitoring by recording the leakage current value on the memory card or in the supervisory system).

Currently, papers on the new numerically advanced methods of determining the active component are still being published. A review of the older and more innovative ideas is included in publications [22,23]. The work [22] lists innovative extensions created after establishing the content of Appendix D of the standard. These include works [24–28], which analyze various techniques for analyzing the current signal—both with only the total leakage current and additionally with a separate resistive component, allowing the amplitude and shift angles in the current signal for the components to be obtained—total and/or resistive [24–26], as well as leading to the determination of the shape and similarity of current signals recorded in a synchronous manner [27,28]. On the other hand, in the work [23], a number of improved classical methods have been compiled that allow its resistive component to be obtained from the current signal, specifying the limitations of their use, of which the presence of higher harmonics in the supply voltage was indicated in the first place.

New methods of determining the resistive components and their practical applications leading to the online diagnostics of limiters are still described in the literature [29–39]. For example, an interesting solution is the online method of measuring the resistive components proposed in [29], which uses a remote non-simultaneous method of measuring the resistive current (RNS). RNS remotely and non-simultaneously measures all types of resistive current parameters using remote, non-simultaneous phase difference measurement methods and specific harmonic analysis algorithms. The results of the simulation and the application of the proposed method showed sufficient accuracy, also in the conditions of frequency deviations and the presence of harmonic components in the supply voltage, which makes it possible to effectively use it in online diagnostics.

Great opportunities are offered by the machine learning method, which, by determining patterns of clearly defined damage, offers ways to effectively determine the following [27,40]:

- Surface conductivity;
- The deposition of metallic impurities.

For example, paper [40] describes the results of the analysis of surge arresters from operation with a rated voltage of 11 kV (continuous operating voltage 9 kV, rated discharge current 5 kA), which were artificially soiled on the surface using the SLM method described in the IEC 60507 standard [41]. This method uses a spray application of a mixture of NaCl and kaolin dissolved in distilled water. Using different compositions of the spray mixture, the different conductivities of the outer layer were obtained after the process of appropriate drying in a thermal chamber. The correctness of the applied layer in terms of its uniformity was confirmed by using machine learning to detect the dirt obtained at

different concentrations of conductive material (5 levels) and relative humidity levels of 40% and 70%. During aging, an increase in the third harmonic of the leakage current and a decrease in HR, defined as the ratio of the fundamental harmonic to the third harmonic of the leakage current, was observed.

The measurements taken in the field were used to determine the lifetime of the limiters in the software and used in planning repairs. An example is the analysis [42] of the MOSA test results leading to the creation of a model combining ANFIS and the SVR model used at a later stage to determine the remaining life of use. A time series consisting of the leakage current and the value of the third harmonic component obtained from field measurements was used to teach and validate the implemented models. Forecasting models were qualitatively and quantitatively assessed using inspection graphics and an analysis of the adopted metrics for four different time horizons, respectively. In methods of this type, it is important to determine the correct criterion indicating the critical level of the exploited ZnO ceramics, for which physical and chemical tests are necessary, while also taking into account the statistical differences between the output parameters of new arresters and those of elements subjected to aging in complex exposure conditions.

An example of the test results obtained by the authors for two MV and LV oxide surge arresters is presented in Figures 2 and 3, respectively. The dispersion of the obtained values of the active component of the leakage current indicates the extreme variation in production quality and the related difficulties in arriving at unambiguous conclusions regarding eliminating the surge arresters from operation. In principle, this type of work should be carried out on specific control samples each time a batch of surge arresters is put into operation in power plants. This applies in particular to very poor-quality arresters, an example of which is shown in Figure 3. The data collected in relation to the individual technical solutions and manufacturers could be used as reference data for the analysis of the operational results only in the case of observing the stability of the measurement results of leakage currents and reduced voltages. As can be seen from Figure 3, for LV arresters, this kind of preliminary testing should be crucial even in the context of the decision to put the delivered batch of products into operation.

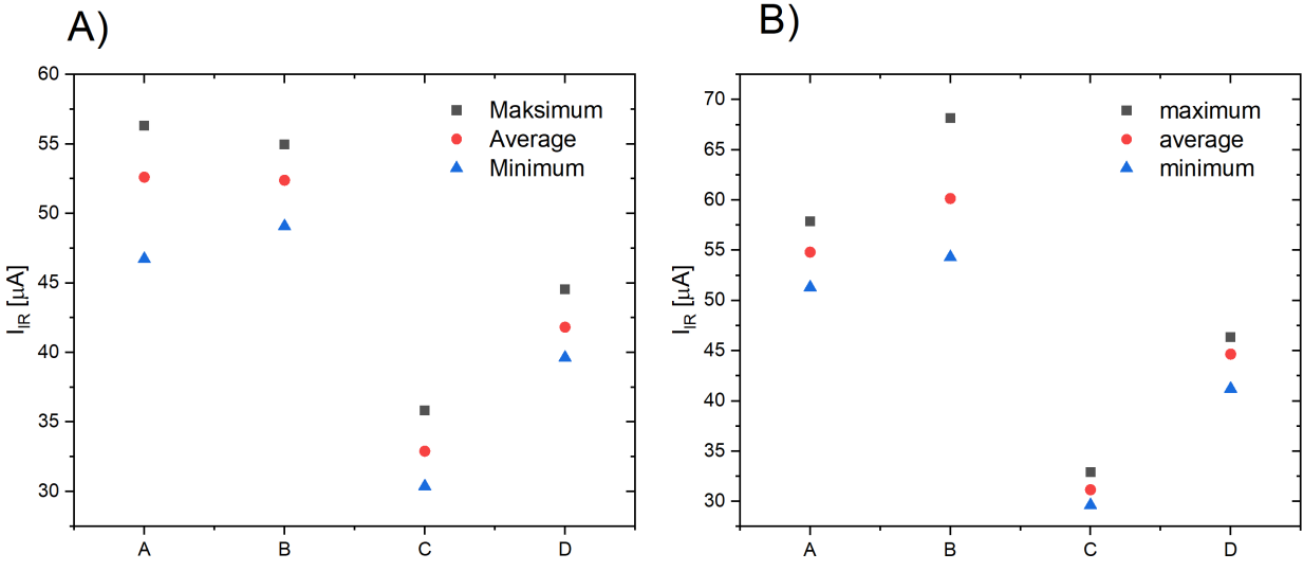

Figure 2. Leakage currents of MV arresters (**A**) new and (**B**) after applying a single current surge, obtained on the basis of testing 10 samples of an arrester with similar-rated parameters from manufacturers A, B, C and D.

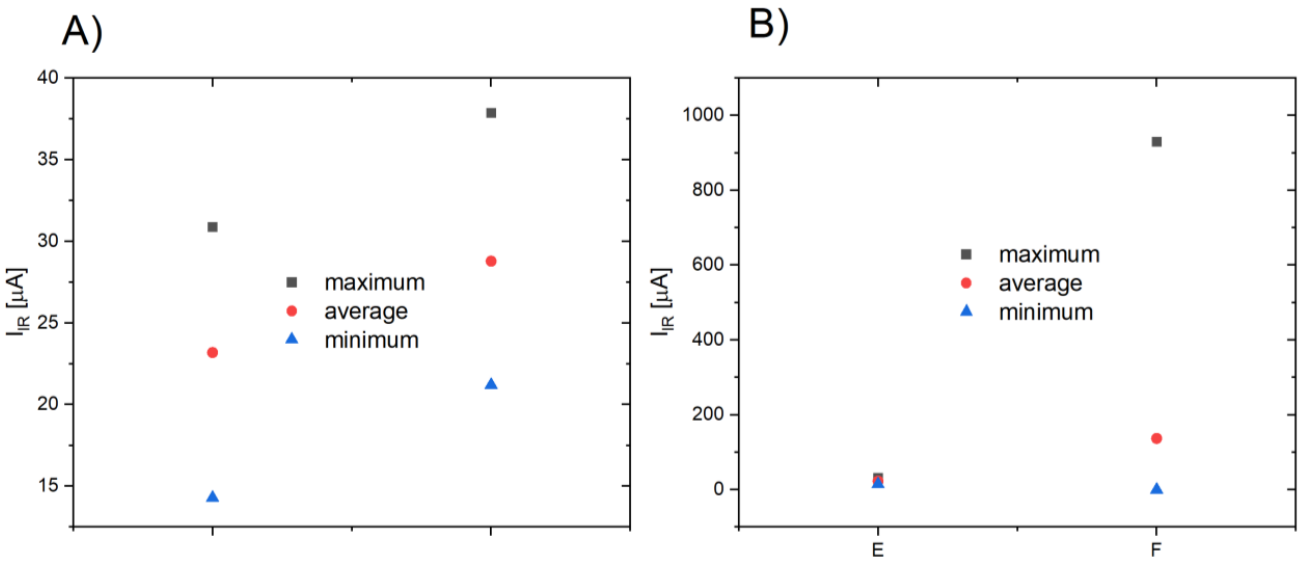

Figure 3. Leakage currents of LV arresters (**A**) new and (**B**) after applying a single current surge, obtained on the basis of testing 10 samples of an arrester with similar rated parameters from manufacturers E and F.

Figures 2 and 3 indicate the need for power plants to perform commissioning tests with independent entities to confirm the repeatability of the basic parameters of the surge arresters used in the power system. Figures 2 and 3 show the results of the active component of the leakage current for a 10-element sample taken from two different manufacturers of MV I LV arresters, respectively. The significant dispersion of the results of the active component of the leakage current shown in Figure 2B for manufacturer B and in Figure 3B for manufacturer F indicates possible problems in ensuring proper overvoltage protection during operation. The specified tests should be supplemented with the measurements of the reduced voltage in order to determine the correct quality of the arrester during operation at the rated discharge current.

In some countries, power utilities use methods for HV surge arresters that measure the following parameters of the leakage current: peak and average values and the content of harmonic components. On the basis of the determined values, the coefficients p_1, p_2 and p_3 are calculated using the Formulas (2)–(4):

$$p_1 = \frac{I_{avg}}{I_{max}} \tag{2}$$

$$p_2 = \frac{I_h}{I_{max}} \tag{3}$$

$$p_3 = \frac{I_{avg}}{I_{max}} \tag{4}$$

which should be included in the range $p_1 \in (0.5; 0.76)$, $p_2 \in (0.01; 0.06)$ and $p_3 \in (0.01; 0.09)$ [43].

If the permissible values are exceeded, it is recommended to disconnect from the mains voltage and measure the leakage current at a DC voltage. In order to check the effectiveness of the above-mentioned method at the deformed mains voltage, when there are high distortions in the leakage current, additional tests can be performed to determine the suitability of the above-mentioned method in extreme operating conditions (e.g., rain and dirt).

3. An Example of the Leakage Current Measurement for HV Surge Arrester

During the tests, measurements of the leakage current of HV surge arresters were carried out using two voltage sources with different contents of higher harmonics. The measurements concerned fully operating overhead surge arresters with a continuous operating voltage of Uc = 77 kV and a rated discharge current of 10 kA.

The tests were carried out using 50 Hz test sets with voltages of up to 150 kV and 300 kV (Figure 4) characterized by a significant distortion of the voltage curve (THD > 10%). The voltage was measured using a WMUT 3 m connected to a capacitive divider, and the current was determined on the basis of the voltage measurement on a non-inductive resistor. Both given values were recorded with the Tektronix TDS 5034B oscilloscope in order to perform the necessary calculations to determine the active component of the leakage current. The oscilloscope's input channels recorded 10,000 samples in 40 ms, from which the current and voltage harmonics were then calculated.

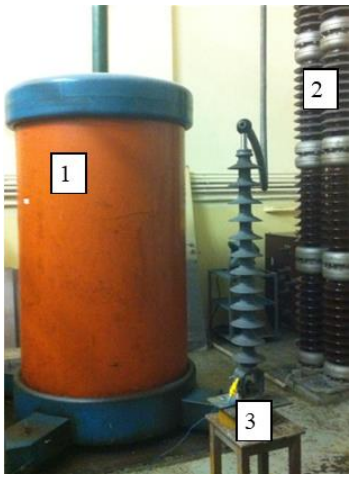

Figure 4. Measuring stand with tested arrester: 1—high voltage transformer 300 kV, 2—voltage divider capacitor, and 3—surge arrester.

In order to determine the technical condition of the six arresters, the leakage current was measured and its resistive component was determined at the continuous operating voltage U_c = 77 kV and the rated operating voltage U_r = 96 kV. In addition, in accordance with the manufacturer's data, the reference voltage of the arrester was checked by reaching the maximum value of the leakage current, which is around 5 mA, which, according to the manufacturer's guidelines, should be within the range of 101.6 ÷ 106.3 kV. In addition, for both test assemblies, the characteristic values were determined in accordance with the methodology proposed by [43]:

- Peak value;
- Average value;
- Harmonic content.

and then the values of p_1, p_2, p_3 were calculated by employing Formulas (2)–(4).

The measurements were aimed at checking the correctness of the measurement of the leakage current with different contents of higher harmonics in the supply voltage and to determine the impact of higher voltage harmonics on the obtained test results. A comparison of the test results of the limiter with a dry surface and during the influence of artificial rain was also made.

A summary of the measurement results on two test assemblies with a significant and different content of higher voltage harmonics is shown in Table 1. Even with a significant content of higher harmonics, the p_1 indicators of the technical condition of the arrester are limited. On the other hand, the remaining p_2 and p_3 indices concerning higher harmonics clearly exceed the acceptable levels given in [43].

Table 1. Results of measurements and calculations of characteristic values of the leakage current for arresters.

Leakage Current Parameter	Test Stand A		Test Stand B	
	U = 77 kV THD$_U$ 13%	**U = 96 kV THD$_U$ 11%**	**U = 77 kV THD$_U$ 21%**	**U = 96 kV THD$_U$ 18%**
Peak value I_{max} [µA]	678.8	1021.9	948.9	1328.5
Average value I_{avg} [µA]	408.4	597.8	491.1	779.0
Harmonic content I_h [µA]	171.5	308.1	415.2	510.4
p_1	0.60	0.58	0.52	0.59
p_2	0.25	0.30	0.44	0.38
p_3	0.42	0.52	0.85	0.66
I_R [µA]	43.6	247.18	172.36	408.17

Large distortions of the voltage curve cause a strong increase in the current harmonics of higher orders, which causes a significant increase in the value of the leakage current, including its active component. The calculation of the actual value of the active component of the leakage current additionally requires knowledge of the frequency characteristics of the arrester, which allows for the compensation of dominant harmonic components. The given example of leakage current measurement indicates the need to introduce advanced numerical analyses that will enable the determination of the active component in reference conditions.

The technical conditions of the tested six surge arresters are similar. Figure 5 shows the level of the leakage current and its active component measured with the test unit B for the unit with a THDU of 20%. With a high content of the third harmonic in the supply voltage, for individual arresters, the active component of the leakage current, with a small dispersion of the measured values, maintains a relatively low value up to and including the continuous operating voltage. For the tested limiters, a change in the I(U) characteristic is observed after exceeding the voltage U_c, which is related to the increase in the resistive component in the leakage current (Figures 6 and 7). In addition, the RMS values of the voltage at the leakage current amplitude of 5 mA are in accordance with the requirements of the arrester manufacturer, which gives their correct technical condition.

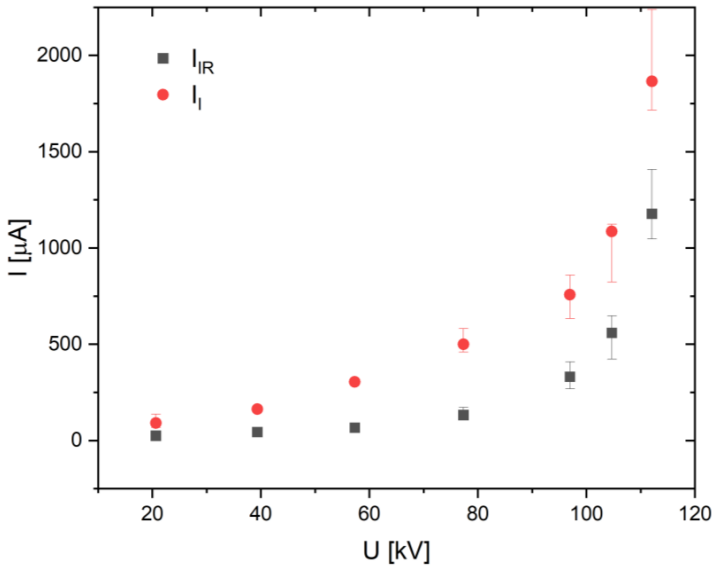

Figure 5. Current–voltage characteristics for the 6 tested arresters in the range of leakage current (average, maximum and minimum values of leakage current are marked) in the conditions of supplying unit B.

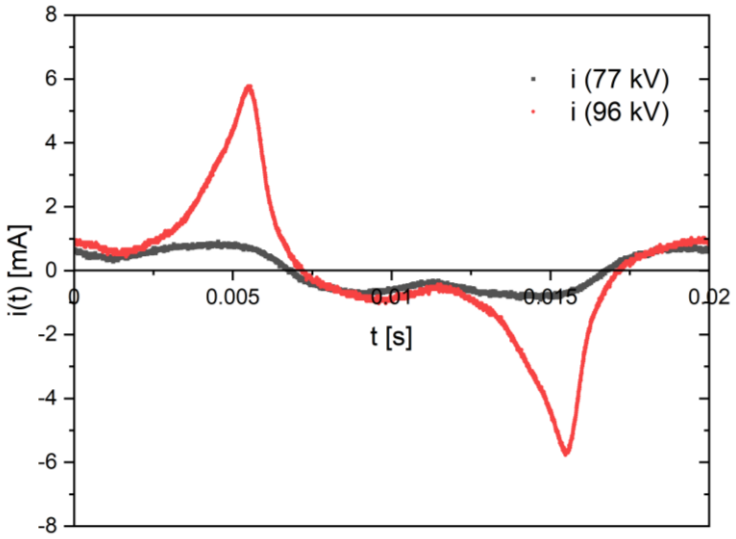

Figure 6. The course of the leakage current of the arrester No. 4 measured at the voltage Uc = 77 kV and Ur = 96 kV with the power supply conditions of the test unit A.

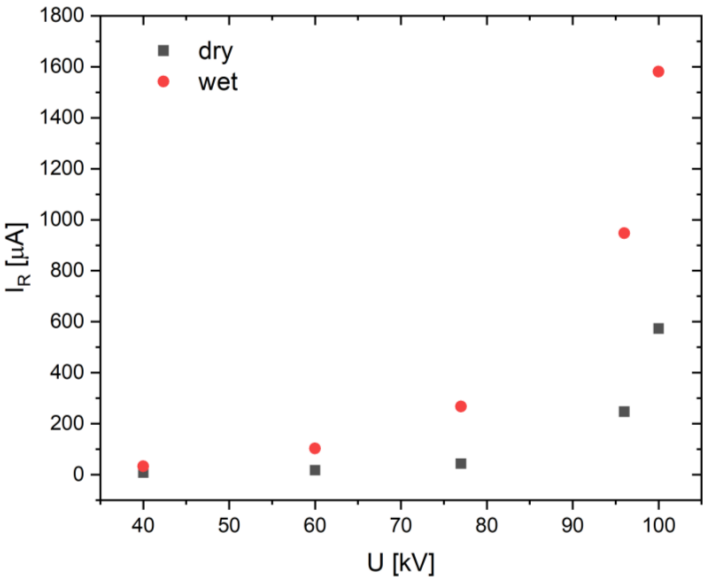

Figure 7. Influence of the surface condition of the arrester No. 4 on the value of the resistive component of the leakage current.

The comparison of the measurement results of the arrester with a dry and wet surface shows several times higher values of the active component of the leakage current in conditions of artificial rain (Figure 7).

4. Errors and Their Correction in Determining the Active Component of the Leakage Current

In order to correctly determine the active component of the leakage current, it is easiest to calculate its value using the appropriate measurement procedures only on the basis of the leakage current oscillogram. For this purpose, various algorithms are used, among which the shift method [30,36] and orthogonal vectors [44] should be mentioned. In operational applications, the current of the arrester is measured using current clamps with specific frequency characteristics that allow for the proper calibration of the measuring systems and determination of the measurement errors. It should be remembered that for diagnostic purposes, small currents of the order of several tens to several hundred µA are measured, usually in interference conditions, e.g., in the case of HV line surge arresters, when we

are dealing with corona and a relatively high electric field strength near the ground [34]. The measurements carried out by the author analyze the following technical problems that occur when measuring leakage current:

- Angular and amplitude errors of commercial current clamps used to measure the leakage current in surge arresters;
- Angular and amplitude errors of voltage transformers used in MV lines;
- Measurement uncertainties related to the characteristic disturbances in the current signal related to the properties of the ZnO arrester and the influence of temperature, voltage amplitude and shape, as described in more detail later in this work.

4.1. Metrological Properties of Current Clamps

In order to correctly determine the leakage current of the arrester and its components using the clamp method, it is necessary to determine the amplitude and phase errors of the measuring transducers used in the frequency range of at least 5 kHz.

The selected frequency range results from the content of higher voltage harmonics typical for power systems, the permissible level of which results from the regulations and the standard [45] related to the issue of electricity quality. As a standard, the THD level in the supply voltage is up to 8% in LV and MV networks for voltages not exceeding 36 kV. The harmonic distortion factor, THD, and the voltage harmonic percentage level are given by relations (5) and (6).

$$\mathrm{THD} = \sqrt{\sum_{h=2}^{40} u_h} \tag{5}$$

$$u_h = \frac{U_h}{U_1} \text{ for } h \geq 2 \tag{6}$$

The permissible levels of harmonic components up to the 25th order specified in the standard are the same (Figure 8), and the highest values are observed for the 3rd, 5th and 7th harmonics, which should not exceed 5%, 6% and 5%, respectively. The levels of current harmonics recorded during electricity quality measurements are much higher and depending on the distortion and short-circuit power of the supply voltage source and the type of non-linear receiver, the THD factor in the load current may reach much higher values, even in the order of several dozen percent.

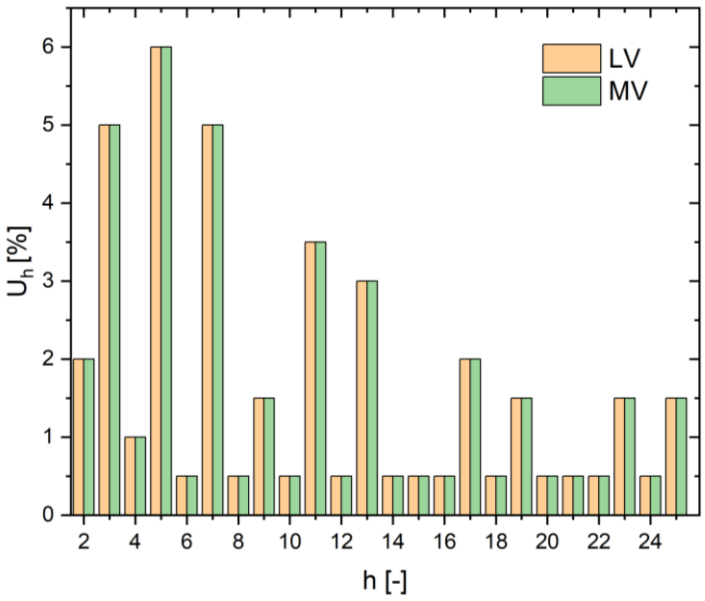

Figure 8. Permissible levels of harmonic components in LV and MV networks [35].

The scaling of the clamps with a sensitivity of 1 µA used in the measurements was performed for frequencies in the range up to 20 kHz in the system shown in Figure 9. Before scaling, a routine calibration of the oscilloscope's measurement inputs was carried out and AC coupling was set in all its channels. In addition, the lack of phase shifts between the inputs was checked. The combination of the calibration systems allows you to immediately assess certain metrological properties of the ALCL-type current clamps used. The documentation provided by the manufacturer indicates that the clamps obtain an output voltage signal depending on the input resistance of the oscilloscope input, which is 1 MΩ as the standard for the device used.

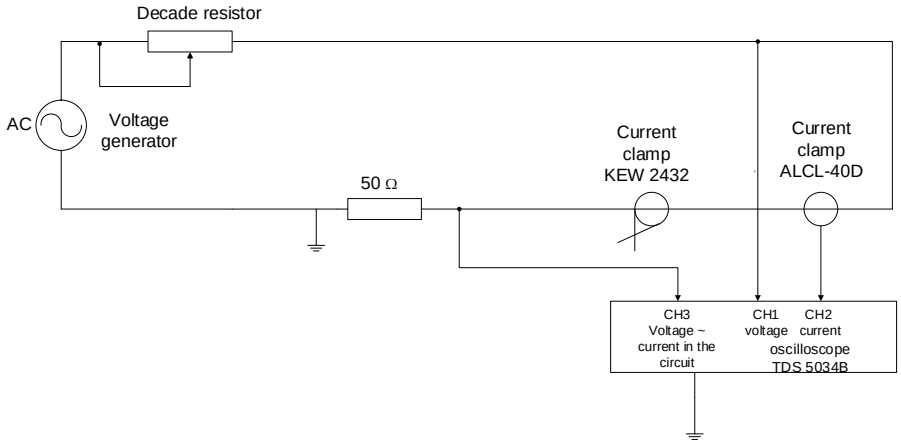

Figure 9. Scheme of the measuring stand for current clamp calibration.

According to the characteristics provided by the manufacturer (Rated Primary Current AC50A, Applicable Current 1 µA~50 A, Max. Capable Current 60 A, Nominal CT Ratio 2400:1, CT Inside Diameter φ37 mm), a significant sensitivity of the clamps was obtained but unfortunately with the incorrect transmission of the higher harmonics of the measured signal. The above clamps have the characteristics of the output voltage as a function of the current measured in the cable, given by the manufacturer, depending on the load resistance of their output. Based on this characteristic and the measurements of currents in the range of 10–800 µA, it was found necessary to introduce a higher resistance than 1 kΩ. By comparing the results of the current measurement at three different frequencies, 50 Hz, 150 Hz and 250 Hz, with the ALCL-40D clamps and the voltage recorded at the shunt terminals, it was finally decided to use the parallel resistance of 100 kΩ, which shifts the U(I) characteristics of the clamps towards lower values and ensures its linearity in the expected range of currents. For the above load, the linearity of the U(I) characteristic in the range of 10–800 µA was obtained for the three given frequencies with the coefficient $R^2 > 0.9976$. In addition, the central position of the wire in the clamps should be maintained in order to obtain repeatable test results.

Due to the fact that the leakage currents of the surge arrester increase approximately proportionally to the frequency, it may turn out that with a significant content of high order harmonics, the calibration factor specified only for the fundamental frequency will cause significant errors in the measurement of the leakage current, overstating the final result. In addition, using the algorithms for determining the active component of the leakage current, the correction time shifts introduced in the clamp measurements will cause additional errors.

Figure 10 shows the recorded voltage signals from the calibrated clamps (oscilloscope channel 2) and the voltage drop across the non-inductive series resistance in the circuit (oscilloscope channel 3) with a sinusoidal signal with a frequency of 50 Hz set on the power generator. The voltage signal from the current clamp clearly precedes the reference signal coming from the non-inductive resistor. For the waveform defined in this way, the amplitude calibration factor can be determined as the current in the circuit related

to the output voltage signal of the clamps, and the phase calibration factor as the phase shift between the voltage waveforms coming from the current clamps and the voltage drop across the non-inductive resistor. The waveforms of the above-mentioned calibration coefficients significantly depend on the frequency, which is shown in Figures 11 and 12, respectively.

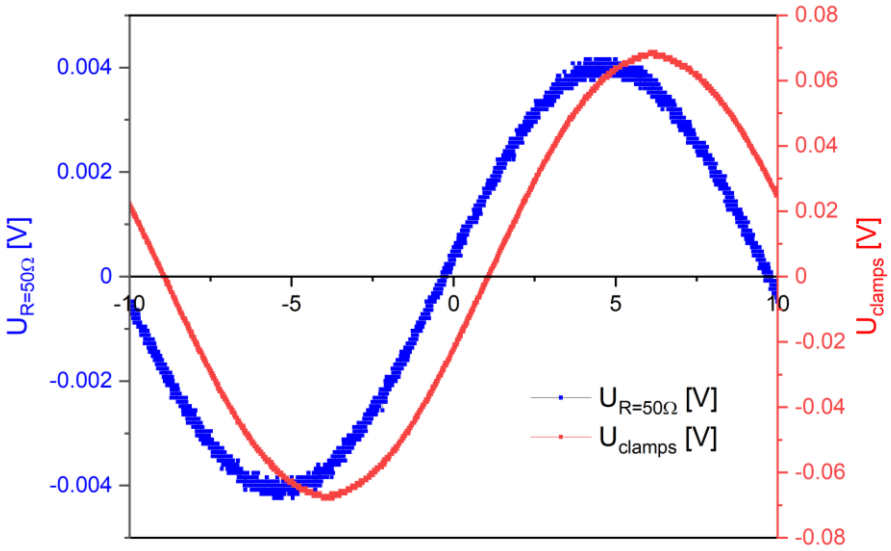

Figure 10. Voltage waveform from current clamp, U_{clamp}, and non-inductive resistor, $U_{R=50\Omega}$.

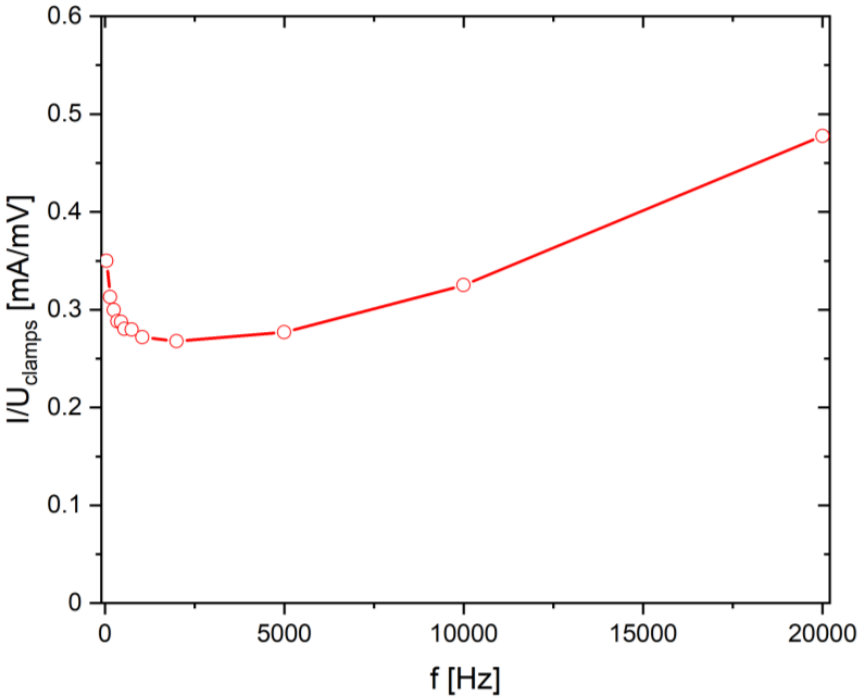

Figure 11. Amplitude calibration coefficient is determined by the ratio of the current in the circuit to the voltage generated at the output of the clamps.

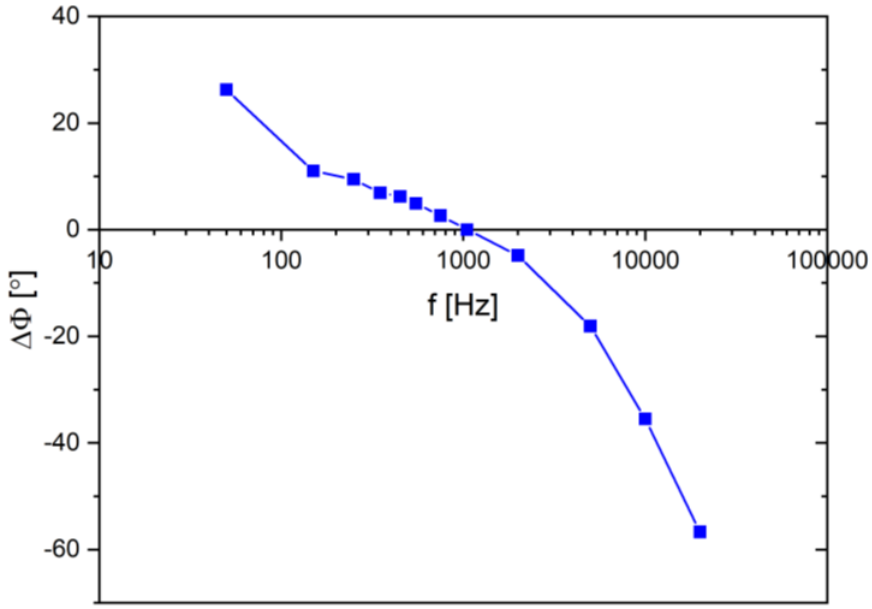

Figure 12. Phase calibration coefficient determined by the shift of the clamp signal in relation to the real signal.

The frequency response shown in Figure 12 shows that the voltage signal produced by the clamps up to 1 kHz reaches the actual current in the circuit and then lags behind. On the other hand, the characteristic of transferring the current values from Figure 11 by the clamps is strongly non-linear, with a minimum frequency of 2 kHz. Both operation at low frequencies and then for higher current frequencies above 5 kHz cause a reduction in the voltage signal, resulting in the need to introduce higher coefficients to be converted into the correct output value corresponding to the actual current in the circuit. The quite complicated characteristics of the clamps show that the conversion of the signal recorded with the above method in technical measurements requires, initially, a decomposition of the signal into higher harmonics, a conversion of the component signals using appropriate amplitude and phase correction factors, and then assembling the signal into a real one, which can, for example, be implemented programmatically in the Labview software.

It should be noted that, in relation to the direct method of measuring the voltage drop on the reference resistor with an oscilloscope, other methods give several percent errors resulting from the data processing algorithm in analog-to-digital converters (Figures 13 and 14). It seems that with the nature of the voltage signal in the clamps, the best results can be obtained by averaging the samples obtained in subsequent periods and using calculations in accordance with the principles of theoretical electrical engineering.

The results of the leakage current measurements using the current inputs of the PK1 and PK2 multimeters, shown in Figure 14, indicate small errors in relation to the method treated as the standard one. However, the use of commercial PK-C current clamps may cause large errors when working with signals with frequencies exceeding 2 kHz (Figure 13). Figures 13 and 14 show a comparison of the leakage current results obtained using the direct method and the indirect method using commercial current clamps. During the measurements, a power generator forcing frequencies up to 20 kHz was used, characterized by a negligible content of higher harmonics. Despite this, current values were obtained from clamp measurements with satisfactory accuracy at frequencies up to about 1000 Hz. Perhaps this is a result characterized by a specific technical solution for the clamps. However, this indicates the problem of assessing measurement accuracy using the indirect current method, so it should undoubtedly be suggested in diagnostic measurements to check the metrological properties of the clamps in advance in order to avoid erroneous conclusions.

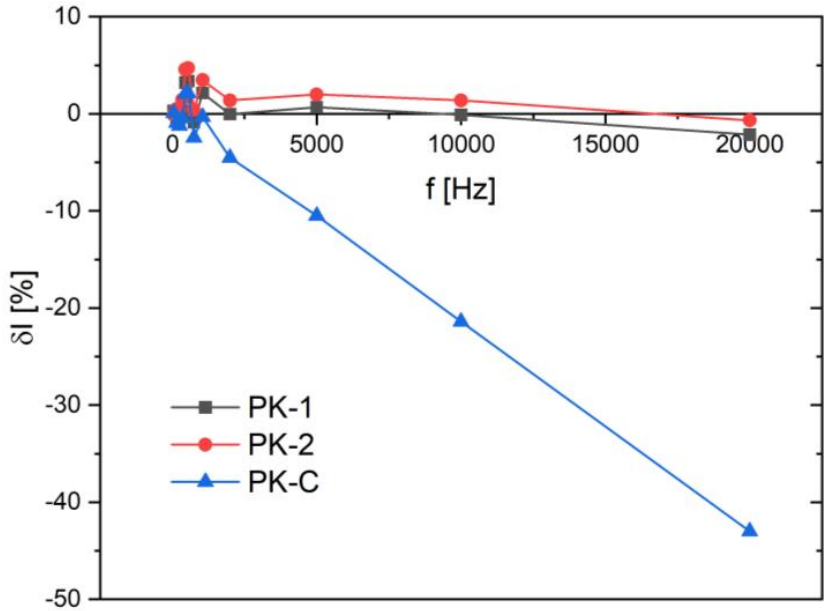

Figure 13. Amplitude error of current measurement for commercial meters in the range up to 1 kHz (PK1, PK2—commercial instruments with voltage measurement function, PK-C—clamp meter with a sensitivity of 1 μA).

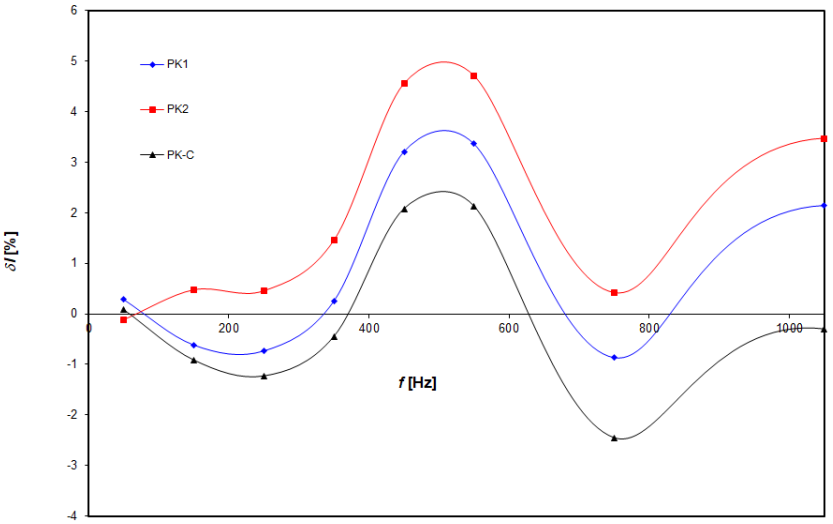

Figure 14. Amplitude error of current measurement for commercial meters in the range up to 1 kHz (PK1, PK2—commercial instruments with voltage measurement function, PK-C—clamp meter with a sensitivity of 1 μA).

4.2. Analysis of the Properties of Voltage Transformers

Similar problems as described in Section 4.1 occur when voltage transformers are used for oscillography or voltage measurement in power systems and also on surge arresters in order to more accurately calculate the active component. Voltage transformers in power measurement systems ensure the adjustment of the voltage on the secondary side to the standardized requirements of measuring devices, e.g., analog and digital voltmeters or voltage coils of power meters or actuators in protection systems. In the case of unearthed voltage transformers, additional galvanic separation is obtained between the high and low voltage circuits because all parts of the primary winding are isolated from the earth in accordance with the rated insulation level of the device.

The accuracy of the voltage or current transformation of the transformer is determined by its class, which gives the maximum voltage and angular errors only in the range of the rated frequency of the transformer [46,47]. In order to determine the expected errors in the transformation of frequencies higher than the rated one, measurements of the ratio and the phase shift of the signal from the secondary to the primary side as a function of the frequency of the voltage applied to the primary side of the transformer with a ratio of 15,000/100 v/v and class 0.5 were performed. A power generator was used, which produced a voltage of up to 300 V and frequencies in the range of 10 Hz ÷ 20 kHz. Channel 1 of the oscilloscope records the voltage waveform on the primary side, $u_{MN}(t)$, through a voltage probe with a ratio of 1:100, and channel 2 directly measures the voltage, $u_{mn}(t)$, of the secondary winding (Figure 15). The indicated measurements were made at frequencies of 0.05, 0.1, 0.2, 0.5, 1, 2, 4, 6, 8, 10, 12, 14, 16, 18 and 20 kHz, for which the relations $k_U(f)$ and $\phi(f)$ were plotted, as shown in Figure 16.

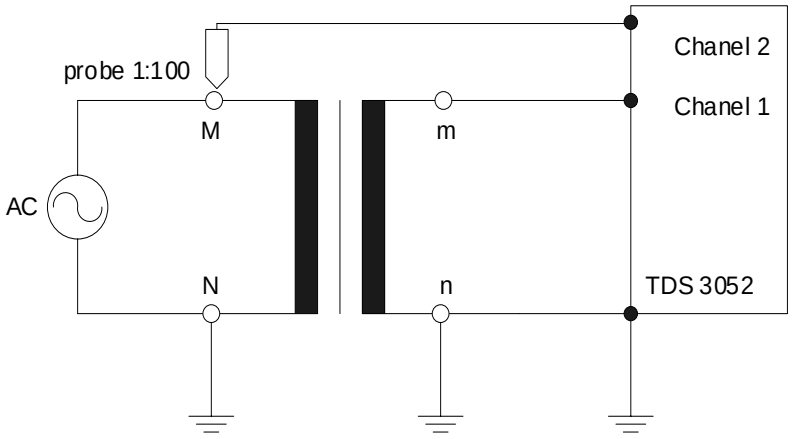

Figure 15. Measuring system for analysis of voltage transformer frequency characteristics.

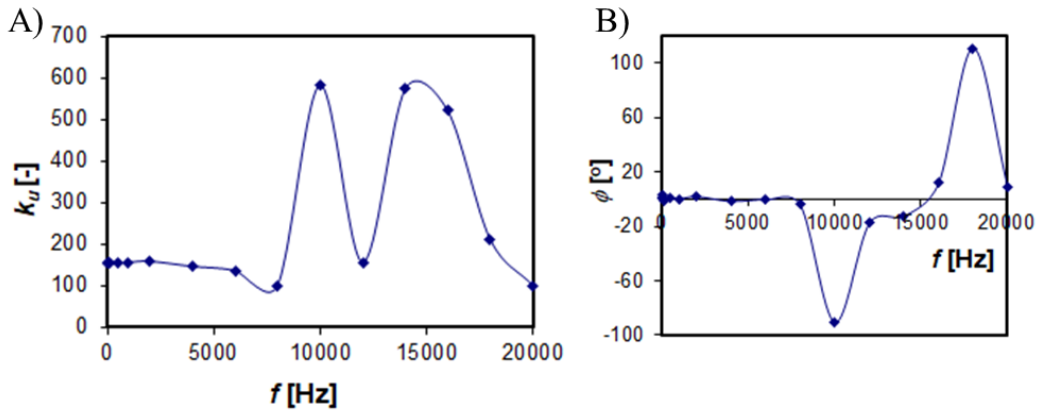

Figure 16. Frequency characteristics of the UMZ20 type transformer: (**A**) voltage ratio; (**B**) phase shift between the voltages of the primary and secondary windings.

On the basis of the performed measurements, it was found that the input signal attenuation occurred at a frequency of about 8 kHz, and for the frequencies of 10 kHz and (16 ÷ 18) kHz, an increase in the ratio resulting from resonance phenomena was found. At the given frequencies, there are strong voltage distortions and a phase shift between the primary and secondary voltages of the transformer. In the given analyzed case, in the frequency range up to 1250 Hz, which is important in mapping the course of typical voltages in power grids, no significant errors were found.

4.3. Correction Factors in Leakage Current Measurements

Leakage current measurements, which are seemingly simple to carry out, require taking into account a number of correction factors, including the influence of temperature—k_T, voltage—k_U and harmonic content (frequency), in order to convert the leakage current to a reference level determined, for example, by a temperature of 293 K, a voltage amplitude U_c and a primary harmonic frequency. In principle, the measurement of leakage current should be abandoned in difficult weather conditions; when in the presence of dew, soot or atmospheric precipitation, the level of leakage current due to significant surface leakage may lead to incorrect conclusions (Figure 7).

4.3.1. Voltage and Temperature Correction Factors in Leakage Current Analysis

In order to obtain correct diagnostic conclusions from the measurements of the leakage current of the ZnO arresters, a number of analyses were performed to determine the impact of the above factors by defining the correction factors: temperature (k_T) and voltage (k_U). These coefficients are necessary to calculate the leakage current of the arrester measured in any voltage and temperature conditions determined by temperature and effective voltage, taking into account the content of higher harmonics. The leakage current is recalculated to the reference level set by the operator in order to unambiguously compare the results of the measurements carried out over a longer time period when changes in both of the analyzed quantities clearly occur in operating conditions. The k_T and k_U coefficients should be determined for a given type of arrester after the leakage current measurements have been carried out in various temperature and voltage conditions [2,48]. Figure 17 shows examples of the k_U coefficients for LV arresters with an operating voltage U_c = 275 V and a rated discharge current of 20 kA with time parameters of 8/20 µs/µs. In addition, the data of the manufacturer of the LCM500 device used in the diagnostics of medium and high voltage limiters, tabulated in [48], have been added. Reference levels of U/U_r = 0.7 and T_w = 293 K are proposed here.

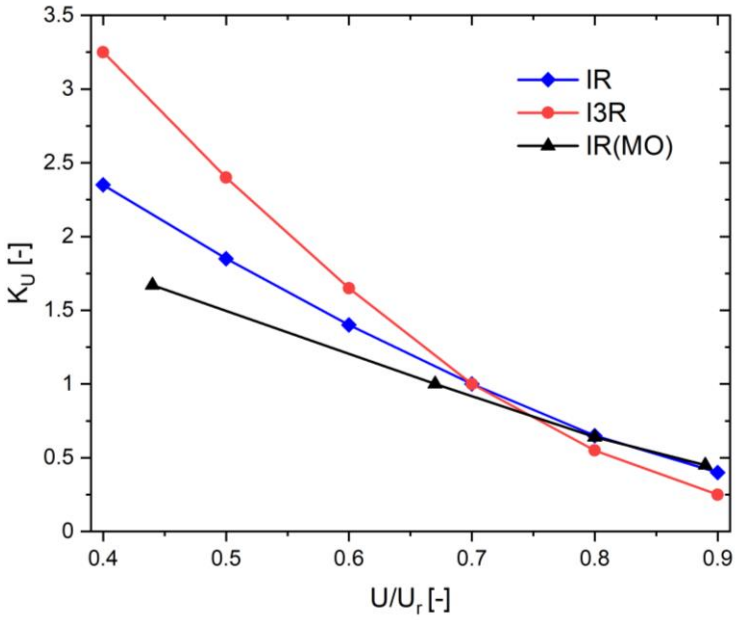

Figure 17. Correction factors [38] taking into account the influence of voltage, IR(MO) and means correction factors, k_U, determined by own measurements.

The correction factors for the LV arresters obtained by our own measurements are similar to those for medium-voltage surge arresters [48] only for the condition of $U/U_r > 0.7$. At the supply voltages, much greater discrepancies were obtained, which may be related to the very small values of leakage currents and additional errors in their measurement.

An increase in temperature causes a decrease in the permanent operating voltage in a manner dependent on the chemical composition of the varistor ceramics [49,50]. With a significant content of iron and aluminum oxides, these changes can be even several times for the selected temperature [51]. Common temperature coefficients, K, defined by Formula (7) in [52] are given at the level of $(0.5 \div 1) \cdot 10^{-3}$/K:

$$K = \frac{\Delta U}{U \cdot \Delta T} = \frac{U_{Tw}(1\ mA) - U_{T0}(1\ mA)}{U_{T0}(1\ mA) \cdot (T_W - T_0)} \quad (7)$$

where:

- U_{Tw} (1 mA)—voltage at T_w and a current of 1 mA;
- U_{T0} (1 mA)—voltage at T_0 and a current of 1 mA;
- T_w—temperature of the surge arrester;
- T_0—temperature at the reference level, equal to 293 K.

For most surge arresters in proper technical conditions, the voltage at the forced leakage current with a temperature increase of 20 K decreases by about 1% [52]. An increased heat release in the varistor structure affects the voltage at its terminals and reduces the permissible levels of current and energy surges as a function of temperature.

Changes in the conductivity of the varistor structure, γ, measured at the reference voltage, $U_{1\ mA}$ (as well as its temperature coefficients), occur according to different band characteristics [50,53]. It turns out that the influence of the chemical composition on the $\gamma(1/T_w)$ characteristic is a complex model containing several partial conductivities in a series–parallel system. However, regardless of the chemical composition of the varistor, the function describing the conductivity of the varistor from its leakage current is correctly approximated by the power function, $\gamma = aI^b$, with constants a and b [50].

Another method, more often used in practice, is to determine the value of the leakage current, $I(U_c)$, at the voltage of the continuous operation of the arrester, U_c, and then to calculate the temperature coefficients, k_T, which are directly converted to the reference temperature, e.g., 293 K, according to Equation (8):

$$I_{T0}(U_c) = k_T \cdot I_T(U_c) \quad (8)$$

In order to determine the correction factors, ZnO varistors from two manufacturers, A and B, were used. In one case, the tests concerned eight surge arresters with a continuous operating voltage of 275 V from manufacturer A. In the second case, varistors (10 pieces of each type) from manufacturer B were tested with a voltage of 0.28 kV, 0.5 kV, 1 kV and 3 kV. The surge arresters were stored in the thermal chamber for 5 h until the temperature distribution in the varistor structure was normalized, and then the current–voltage characteristics were measured in the system with the correctly measured current, forcing a direct or alternating voltage coming, in the second case, from a sinusoidal voltage generator with a low content of higher harmonics.

The correction factors were determined in two operating states: at direct voltage (manufacturer A and B) on the basis of standard current–voltage characteristics and at alternating voltage (only manufacturer A) by determining the resistive component of the leakage current according to the methodology described in [54].

Figure 18 shows the exemplary current–voltage characteristics of the tested surge arresters at the continuous operating voltage, U_c = 275 V, the rated discharge current, 20 kA, and a time parameter of 8/20 µs. Above the DC voltage corresponding to the amplitude of the continuous operating voltage, a slight effect of temperature on the leakage current level is observed.

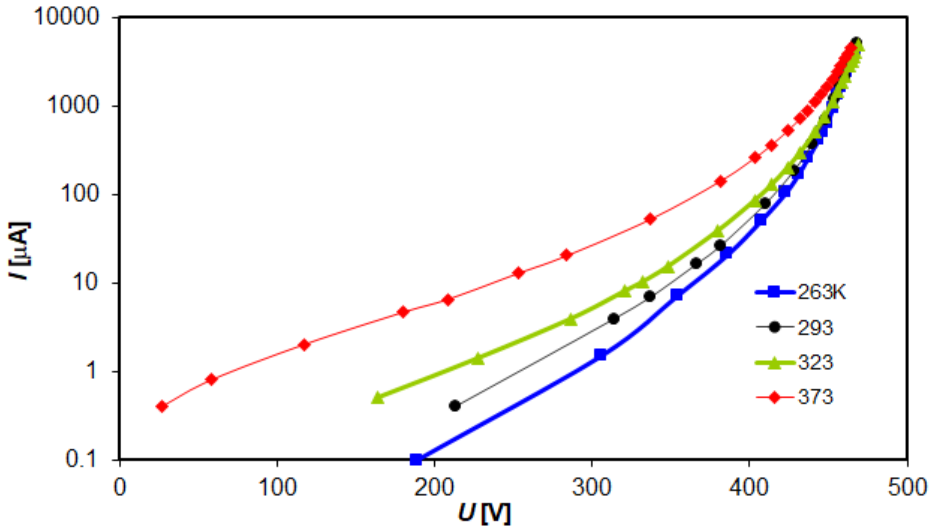

Figure 18. I(U) characteristics for direct voltage of an exemplary surge arrester from manufacturer A.

On the basis of the measured I(U) characteristics, the k_T coefficients for direct voltage, shown in Figure 19, were calculated. These coefficients for the varistors from manufacturers A and B, marked for similar continuous operating voltages, are significantly different. The determined correction factors, especially at low ambient temperatures, are characterized by a significant dispersion of the current value results.

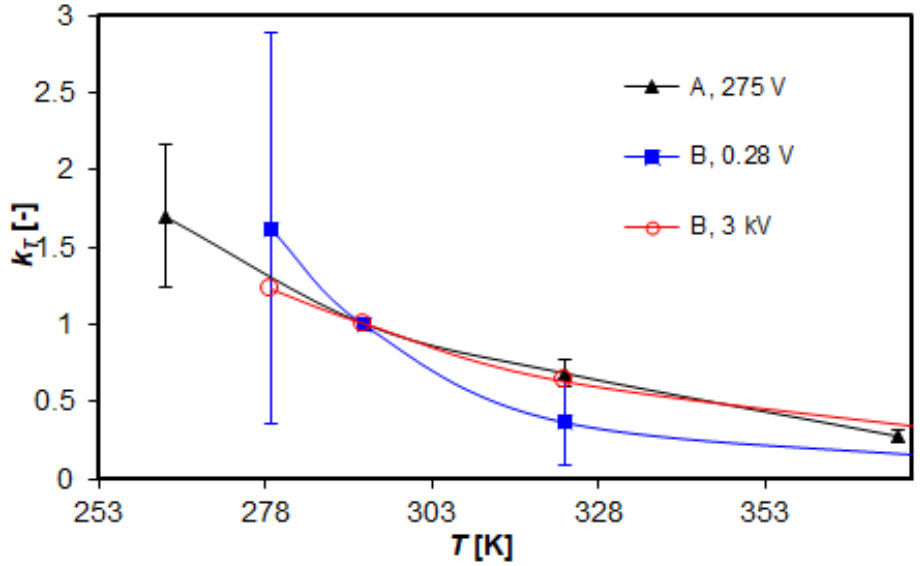

Figure 19. Temperature correction factors calculated from measurements at DC voltage to convert leakage current measurements to reference conditions for T_w = 293 K.

For surge arresters from manufacturer A, the course of the $k_T(T_w)$ coefficient was additionally determined from the measurements of the active component of the leakage current at an alternating voltage, which are similar to the data given in [48] for the temperature range (263 ÷ 303) K. For higher temperatures, slightly higher values of the coefficient k_T were observed, which may result from the properties of the tested ZnO ceramics (Figure 20).

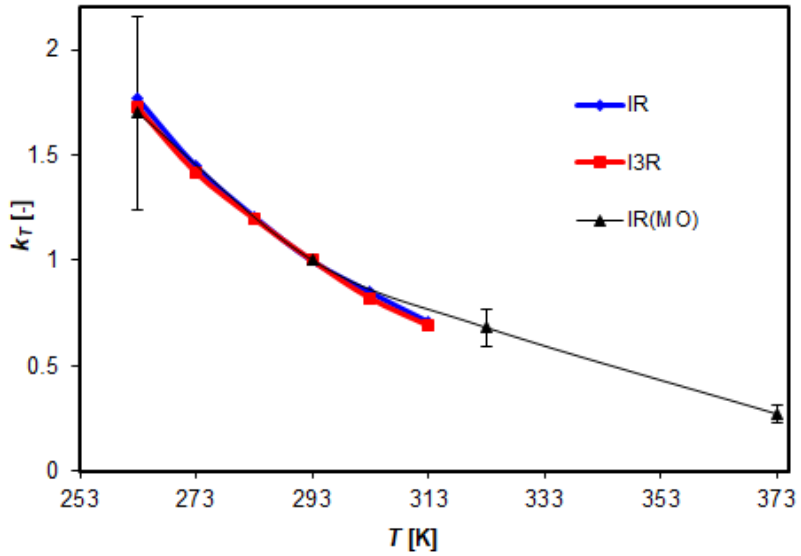

Figure 20. Comparison of leakage current measurements at alternating voltage, I_R, I_{3R}—resistive component and its 3rd harmonic for leakage current according to [2,48]; $I_{R(MO)}$—active component of leakage current determined by own measurements for manufacturer A.

The data from the publication [55] show that, with the identical chemical composition of materials, a change in the temperature profile of the sintering process leads to visible differences in the pre-breakdown characteristics only in the field of tests performed at direct voltage. It follows that the determination of temperature and voltage coefficients should be performed with alternating voltages.

Figure 21 compares the impact of the arrester dimensions related to the continuous operating voltage, U_c, on the course of the temperature coefficient, k_T. The increase in the voltage U_c and thus the volume of the varistor significantly reduces the influence of temperature on the leakage current, which is indicated by the flatter $k_T(T_w)$ characteristic.

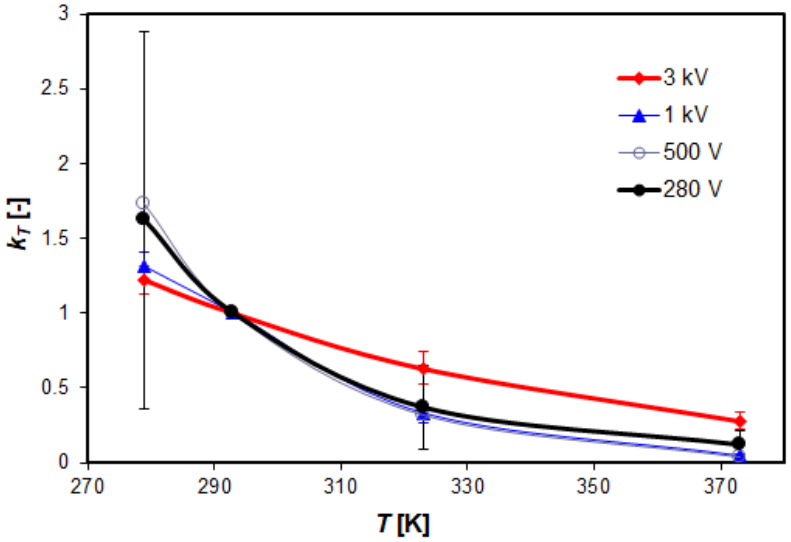

Figure 21. Influence of the dimensions of the arrester from manufacturer B (the height of the varistor is for 280 V—3.5 mm, 0.5 kV—5 mm, 1 kV—8 mm and 3 kV—25 mm) on the value of the k_T coefficient.

4.3.2. Correction Due to Higher Voltage Harmonics

Figure 22 shows the shape of the voltage and current of the arrester, respectively, when the mains voltage is lower than the continuous operating voltage, $U < U_c$, and there is a small level of resistance from the resistive component, but with a significant distortion of

the current waveform due to the higher harmonics of the supply voltage, which originate from the non-linear properties of varistors.

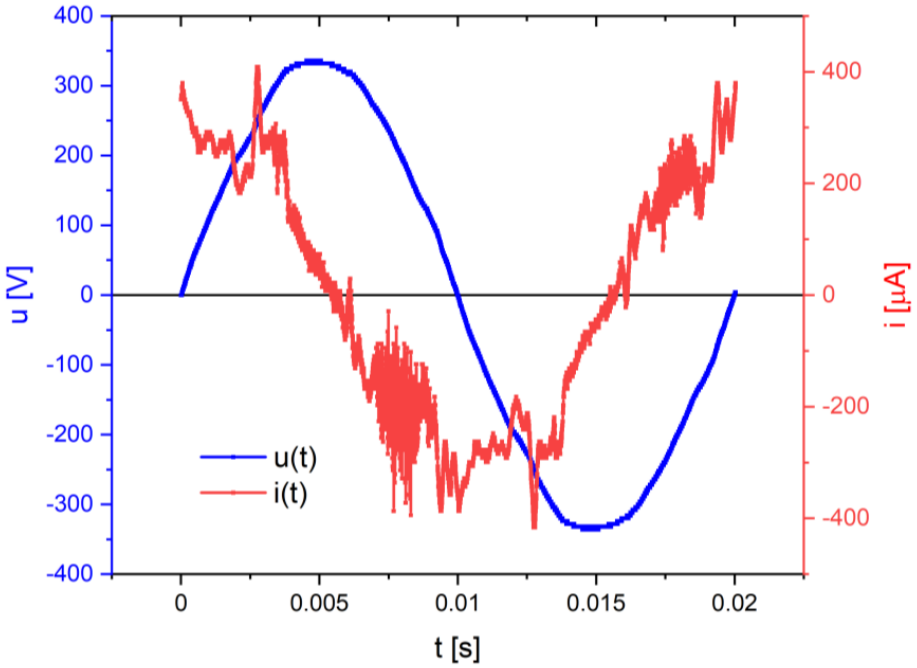

Figure 22. Leakage current, i(t), of surge arrester No. 8 measured at mains voltage, u(t), with RMS value of 237.9 V.

In order to determine the influence of the harmonic frequency of the voltage on the value of the leakage current for the tested surge arresters, the results of the I(f) characteristics tests were used, on the basis of which the characteristics of the module z(f) and the displacement angle φ(f) of the arrester impedance for voltages in the range from 150 to 340 V were calculated.

The impedance characteristic of the limiter enables the introduction of a correction for the content of higher harmonics by implementing the following algorithm:

- Calculation of the content of higher harmonics, u_k and i_k, in the supply voltage, u(t), and leakage current, i(t), respectively;
- Calculation of theoretical, higher harmonics of the leakage current, i_{tk}, and phase, φ_{tk}, based on the previously determined characteristics, z(f) and φ(f), and the FFT (fast Fourier transform) algorithm for the supply voltage;
- Correction of the amplitude of higher harmonics in the leakage current according to the i_k-i_{tk} action;
- Phase correction for odd higher harmonics of the leakage current according to the action of the action $\varphi_k + \varphi_{tk}$;
- Reconstruction based on the corrected values of the amplitude and phase of the i_{cor}.

The correction of higher harmonics, which allows the waveform of the corrected leakage current, $i_{cor}(t)$, to be obtained, can occur for all lines of higher harmonics, even up to the order of 100, or only for those that cause a significant change in the current of a given harmonic. In practice, due to the dominance of the odd harmonics, the 3rd, 5th, 7th, 9th, 11th, 13th and 15th in the supply voltage, it is sufficient to consider only the listed frequencies (Figures 23 and 24).

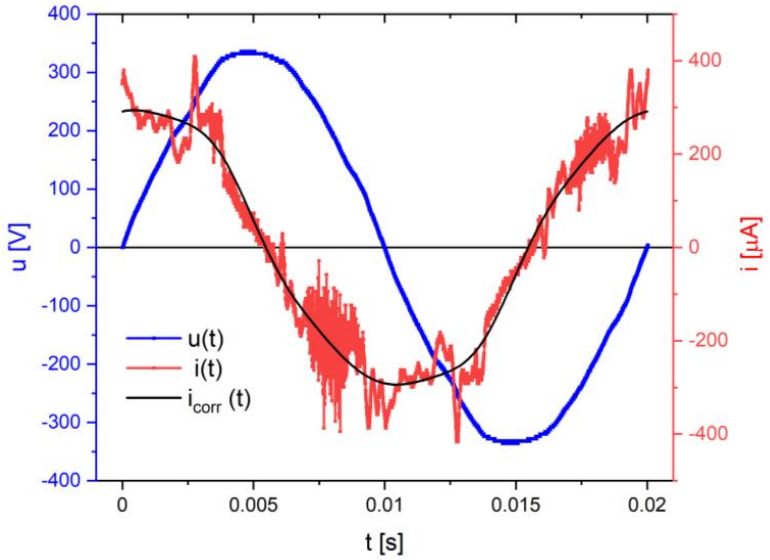

Figure 23. Recorded values of voltage, u(t), and leakage current, i(t), at distorted voltage of U = 237.8 V. The corrected course of the leakage current, $i_{cor}(t)$, was calculated for odd harmonics from 1 to 15.

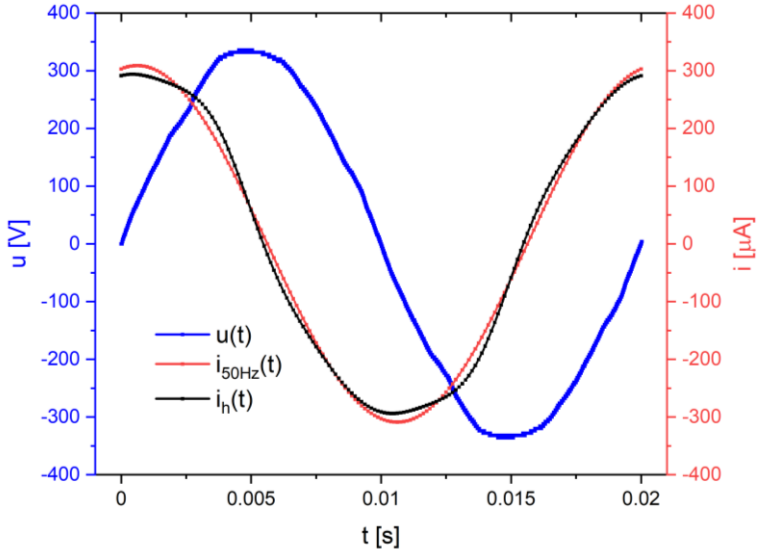

Figure 24. Comparison of the corrected waveform of the leakage current, $i_{cor}(t)$, with the current of the fundamental harmonic at 50 Hz, $i_{50Hz}(t)$, resulting from the analysis with the FFT algorithm of the real waveform, i(t).

It should be mentioned that a varistor in the pre-breakdown state is a capacitive element, which causes the flow of higher harmonics in the leakage current at even small values of higher harmonics in the supply voltage. For this reason, it is necessary to correct the influence of higher harmonics in the supply voltage in order to determine the value of the leakage current in the conditions of a supply with an undistorted voltage. The level of current harmonics in a varistor (except for components resulting from voltage harmonics $i = C \frac{du}{dt}$) depends on its dimensions and the chemical composition of the varistor ceramics, which has a significant impact on its capacity. In addition, the varistor current curve, i(t), contains a number of "interferences" resulting from the measurement of small voltage signals on the shunt or at the output of the current clamps.

The correction of the current waveform occurs up to a frequency of 50 Hz (non-distorted voltage) and allows the leakage current results for the measured surge arresters

to be compared, even with a strongly distorted voltage. The obtained waveform of $i_{cor}(t)$ allows for the correct calculation of the parameters that are important for the assessment of the technical condition of the arrester: the leakage current and resistive component on the basis of active power, according to [54]. The relative error related to the measurement results at an undistorted voltage, in the case of calculating the active component for the corrected leakage current, $i_{cor}(t)$, does not exceed 5%. The proposed concept of correcting the measurements of surge arresters obtained at distorted voltages, provided that the frequency characteristics obtained from the manufacturer for a given type of arrester are available, makes it possible to compare test results and track changes in the leakage current and its active component. This is important for predicting the aging rate of the arrester during its operation.

The proposed method can be used provided that the arrester is supplied with a voltage $U < U_c$ and there is no strong distortion of the leakage current associated with the presence of a resistive component greater or comparable to the capacitive current. In the case of $U > U_c$, the correction is also possible, provided that the impedance characteristic of the arrester with a high value of the active component of the leakage current is available.

4.3.3. Failure to Determine the Leakage Current under Non-Reference Conditions

In order to determine the conversion factor of the measured leakage current value into the actual value, the appropriate correction factors given in Section 4.3 should be taken into account. For this purpose, assuming the correct calibration of the current clamps, the following formula should be used:

$$I_{T0}(U_c) = k_T \cdot I_T(U_c) \tag{9}$$

where coefficients k_U, k_T and k_{THD} result from dependencies (10–12) determined empirically for a selected type of surge arresters.

$$k_U = \frac{I_{U_c}}{I_{U_x}} \tag{10}$$

$$k_T = \frac{I_{293\ K}}{I_{x\ K}} \tag{11}$$

$$k_{THD} = \frac{I_{50\ Hz}}{I_{def}} \tag{12}$$

The k_T and k_U coefficients can be read directly from the appropriate $k_T(T)$ and $k_U(U)$ graphs. These types of data are sometimes provided by manufacturers in data sheets. The results of the tests contained in publications on the influence of ambient temperature on the level of leakage current indicate different waveforms of the value of leakage current measured at different test voltages for a specific type of arrester. For example, for surge arresters with a rated voltage of 120 kV, a 20% increase in the leakage current was found in relation to a reference temperature of 303 K [56]. The k_{THD} factor, on the other hand, depends on the content of individual harmonics during the measurement. In order to calculate it, the algorithm given in Section 4.3.2 should be used. This coefficient can be estimated approximately by giving the ratio of the RMS values of the 50 Hz fundamental harmonic band to the leakage current of the varistor.

A cursory analysis of the dependencies listed in Figures 25–27 allows the maximum additional measurement error introduced during, for example, a temperature of 323 K, to be directly measured.

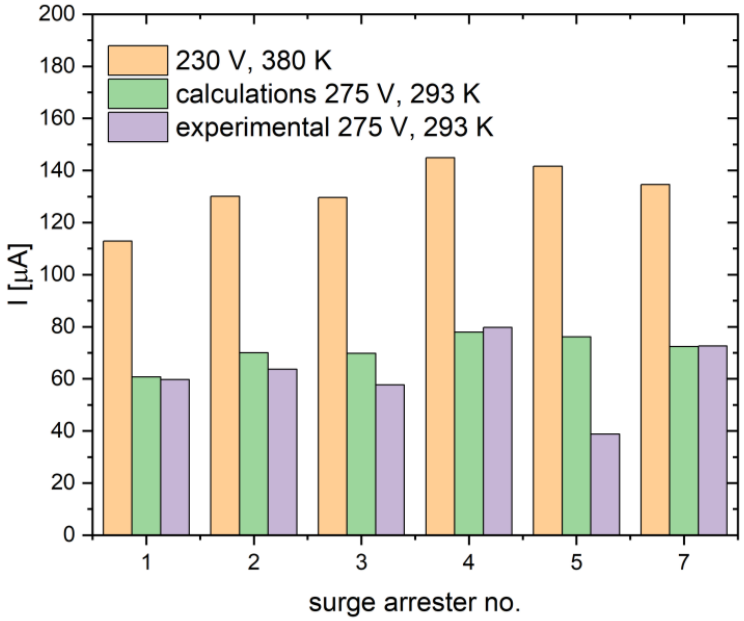

Figure 25. Comparison of the corrected waveform of the leakage current, $i_{cor}(t)$, with the current of the fundamental harmonic.

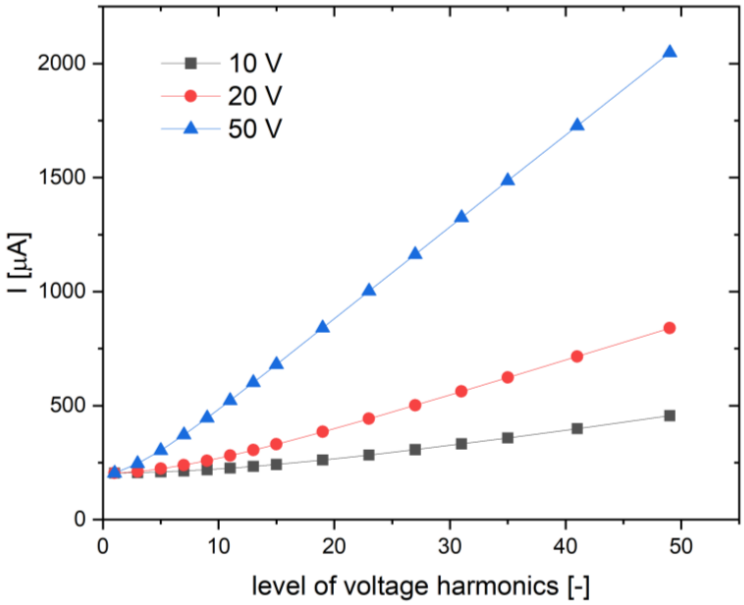

Figure 26. Influence of the level of voltage harmonics on the leakage current of the arrester.

During the error analysis, the leakage current of six low-voltage surge arresters was first measured for different voltages and temperatures. The obtained results made it possible to determine the correction factors, k_U and k_T, for individual surge arresters and the averaged factor, which, in the further part of the analysis, was used to convert the measurement results obtained at a voltage U and temperature T to the reference values, in this case 275 V and 293 K. Due to the different technical conditions of the tested arresters and the dispersion of characteristics being a feature of varistor production, the errors were calculated for the conversion into reference values for individual arresters, which are shown in Figure 28.

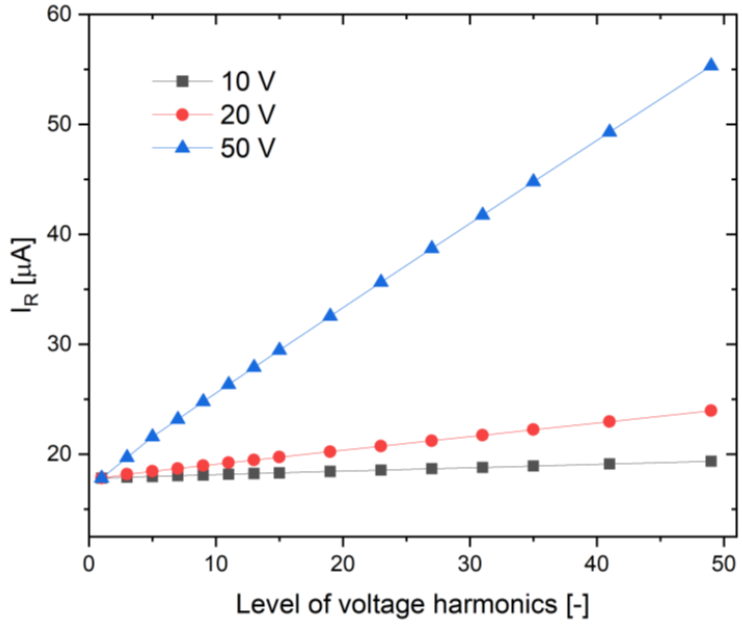

Figure 27. Influence of voltage harmonics on the active component of the leakage current.

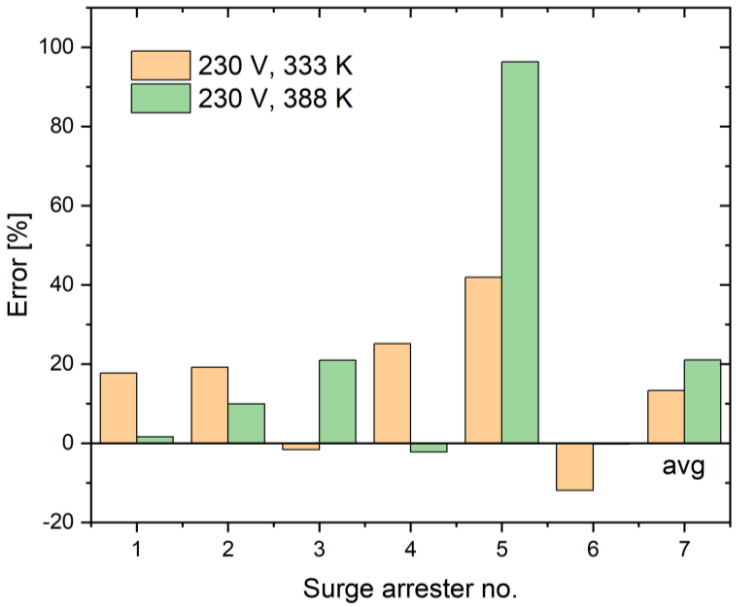

Figure 28. Errors obtained using temperature coefficients when converting measurement results to reference values, U = 275 V and T = 293 K.

In order to determine the influence of higher voltage harmonics on the value of the leakage current, simulations were performed in the Mathcad program using the averaged impedance characteristics of the surge arresters. On their basis, the values of the leakage currents and the active component were calculated during the operation of the arrester at 230 V, on which only one odd harmonic of the order of 3 to 49 with an amplitude of 10 V (4.3%), 20 V (8.7%) and 50 V (21.7%) was imposed. The influence of the phase angle of the superimposed voltage harmonic on the value of the leakage current was also checked.

The results of the numerical analyses obtained indicate that the leakage current of the arrester strongly depends on the frequency of the higher voltage harmonic. The change in the current for a higher harmonic with an amplitude of 20 V imposed on the base waveform with a frequency of 50 Hz increases by as much as 411% from the 3rd to the

49th component. For higher frequencies of the higher harmonic, a significant capacitive component is introduced, which is visible in the leakage current of the arrester (Figure 26).

On the other hand, the active component of the leakage current with the same content of higher harmonics at the level of 8.7%, which exceeds the permissible values in distribution and transmission networks, increases in relation to the 50 Hz component by only 6% (Figure 27).

A simplified correction of the leakage current value may consist of calculating the fast Fourier transform from the waveform of the measured current and calculating the current only from the first harmonic. In addition, with the phase of the electric field strength or the direct supply voltage, you can calculate the phase shift between the current and voltage waveforms for the first harmonic and, on this basis, calculate the active current component in a simplified way. In the case of LV arresters, this procedure gives correct results with an error not exceeding 10%, as shown in Figure 29.

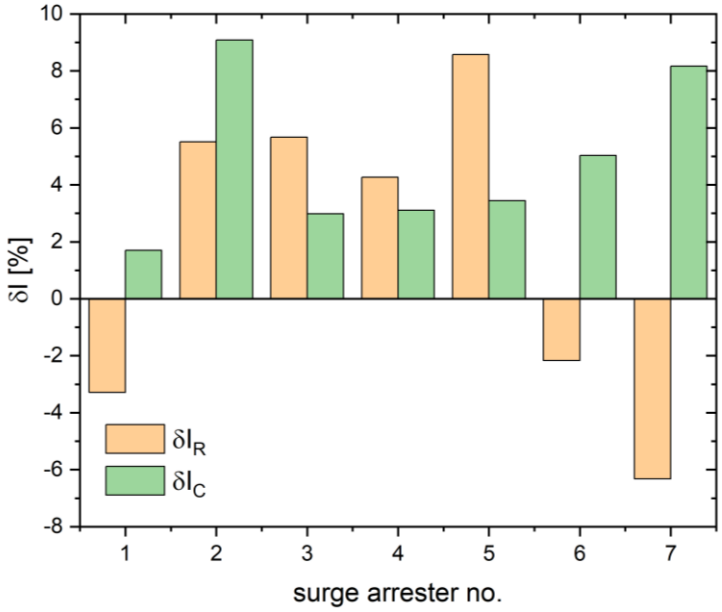

Figure 29. Error in determining the active component, δI_R, and the capacitive component, δI_C, for individual surge arresters on the basis of taking into account the first harmonic of the leakage current.

On the basis of the obtained simulation results, in accordance with the guidelines [57], it is possible to abandon the introduction of correction factors for determining the value of the active component of the leakage current, especially because with an increase in the maximum order of the harmonics in power networks, its amplitude strongly decreases. The permissible contents of the voltage harmonics of higher orders from the 26th and above are not normalized. The guidelines of the standard [45] end on the 25th order, for which the content is required at a level of 1.5%, and for even harmonics of the 6th–24th order, it is 0.5%. The total content of higher harmonics in the supply voltage THD cannot be higher than 8%.

5. Conclusions

Surge arresters, due to the internal structure of varistors, are characterized by a dispersion of the basic parameters characterizing their state in the pre-breakdown state (leakage current and resistive component) and conduction of the rated discharge current (reduced voltages). Tests of the same type of surge arresters, new or used, in this respect provide information indicating the rate of internal aging processes and may be the basis for admitting them for further use.

One of the basic parameters used to assess the technical condition of N operation is the measurement of the current of the active component of the leakage current, with

the possibility of recording the course of the leakage current. This requires the use of a calibrated measurement system based on sensitive current clamps with a conduction band of at least 1 kHz. In addition to ensuring a low level of amplitude and phase error, appropriate methods of signal analysis should be used in the measurements to determine the active component of the leakage current [30,36,44]. However, the determined active component can be considered as a diagnostic indicator only after taking into account the basic factors affecting the level of the tidal current, which include the limiter temperature, mains voltage and the content of its higher harmonics. The determination of the correction factors for the mentioned factors requires experimental knowledge in the field of leakage current measurement in surge arresters of a specific type.

The analyses of the influence of these factors on the measurement error of the leakage current and its active component, performed in the work, indicate that temperature and voltage have a major impact here. The determined correction factors, k_U and k_T, depend on the chemical composition and production process of varistors and their dimensions.

The results of the leakage current measurements of surge arresters, even at $U < U_c$, indicate strong current distortions, even in the range of higher frequencies, usually up to the 15th harmonic, which can be amplified by the presence of harmonics in the supply voltage, indicating the need to introduce appropriate correction factors in order to correctly calculate the current leakage at a fundamental frequency of 50 Hz. Their correct determination is labor-intensive, as it requires laboratory tests to obtain the frequency characteristics of the impedance and phase angle of surge arresters, which only allows for the effective correction of leakage currents measured under distorted voltage conditions.

A simplified solution for correcting the leakage current may be to perform the Fourier transform of the current waveform and perform calculations only for the first harmonic of the current. This is shown by the analysis presented in the final part of the article. However, it should be borne in mind that this type of procedure will be appropriate for a specific type and condition of varistor ceramics. With significant non-linearities in the pre-breakdown state of the varistor, a full analysis of the impact of higher harmonics on the result of the active component of the leakage current should be performed. Another way to avoid a troublesome correction of distortions in the supply voltage is to introduce specific methods for determining the active component of the leakage current [57,58].

Author Contributions: Conceptualization and methodology, M.O.; formal analysis and investigation, M.O., L.S.L. and G.R.; resources, M.O.; data curation, M.O.; writing—original draft preparation, M.O.; writing—review and editing, L.S.L. and G.R.; visualization, L.S.L.; supervision, G.R. All authors have read and agreed to the published version of the manuscript.

Funding: This research received no external funding.

Data Availability Statement: The data presented in this study are available on request from the corresponding author. The data are not publicly available due to legal issues related with privacy of varistors manufacturers.

Conflicts of Interest: The authors declare no conflict of interest.

References

1. Eda, K. Zinc oxide varistors. *IEEE Electr. Insul. Mag.* **1989**, *5*, 28–30. [CrossRef]
2. *EN IEC 60099-5:2018*; Surge Arresters—Part 5: Selection and Application Recommendations. International Electrotechnical Commission: Geneve, Switzerland, 2018.
3. Dobric, G.; Stojkovic, Z.; Stojanovic, Z. Experimental verification of monitoring techniques for metal-oxide surge arrester. *IET Gener. Transm. Distrib.* **2020**, *14*, 1021–1030. [CrossRef]
4. Papliński, P.; Wańkowicz, J.; Śmietanka, H.; Ranachowski, P.; Ranachowski, Z.; Kudela, S., Jr.; Aleksiejuk, M. Comparative Studies on Degradation of Varistors Subjected to Operation in Surge Arresters and Surge Arrester Counters. *Arch. Metall. Mater.* **2020**, *65*, 367–374. [CrossRef]
5. Matsuoka, M. Nonohmic Properties of Zinc Oxide Ceramics. *Jpn. J. Appl. Phys.* **1971**, *10*, 736–746. [CrossRef]
6. Jinliang, H. *Metal Oxide Varistors: From Microstructure to Macro-Characteristics*; Wiley: Hoboken, NJ, USA, 2019.
7. Ott, J.; Lorenz, A.; Harrer, M.; Preissner, E.A.; Hesse, C.; Feltz, A.; Whitehead, A.H.; Schreiber, M. The influence of Bi_2O_3 and Sb_2O_3 on the electrical properties of ZnO-based varistors. *J. Electroceramics* **2001**, *6*, 135–146. [CrossRef]

8. Varastegani, N.; Yourdkhani, A.; Ebrahimi, S.A.S.; Rotaru, A. Varistor and electrical properties of $MgO{\cdot}(Fe_2O_3)1-x(Bi_2O_3)x$ ceramics. *J. Eur. Ceram. Soc.* **2020**, *40*, 1325–1329. [CrossRef]
9. Kim, E.D.; Kim, C.H.; Oh, M.H. Role and effect of Co_2O_3 additive on the upturn characteristics of ZnO varistors. *J. Appl. Phys.* **1985**, *58*, 3231–3235. [CrossRef]
10. Han, J.; Senos, A.M.R.; Mantas, P.Q. Varistor behaviour of Mn-doped ZnO ceramics. *J. Eur. Ceram. Soc.* **2002**, *22*, 1653–1660. [CrossRef]
11. Ma, S.; Xu, Z.; Chu, R.; Hao, J.; Liu, M.; Cheng, L.; Li, G. Influence of Cr_2O_3 on ZnO–Bi_2O_3–MnO_2-based varistor ceramics. *Ceram. Int.* **2014**, *40*, 10149–10152. [CrossRef]
12. Bai, H.; Li, S.; Zhao, Y.; Xu, Z.; Chu, R.; Hao, J.; Chen, C.; Li, H.; Gong, Y.; Li, G. Influence of Cr_2O_3 on highly nonlinear properties and low leakage current of ZnO–Bi_2O_3 varistor ceramics. *Ceram. Int.* **2016**, *42*, 10547–10550. [CrossRef]
13. Pianaro, S.A.; Pereira, E.C.; Bulhões, L.O.S.; Longo, E.; Varela, J.A. Effect of Cr_2O_3 on the electrical properties of multicomponent ZnO varistors at the pre-breakdown region. *J. Mater. Sci.* **1995**, *30*, 133–141. [CrossRef]
14. Watari, T.; Bradt, R.C. Grain growth of sintered ZnO with alkali oxide additions. *J. Ceram. Soc. Jpn.* **1993**, *101*, 1085–1089. [CrossRef]
15. He, J.; Hu, J.; Lin, Y. ZnO varistors with high voltage gradient and low leakage current by doping rare-earth oxide. *Sci. China Ser. E Technol. Sci.* **2008**, *51*, 693–701. [CrossRef]
16. Xu, D.; Shi, L.; Wu, Z.; Zhong, Q.; Wu, X. Microstructure and electrical properties of ZnO–Bi_2O_3-based varistor ceramics by different sintering processes. *J. Eur. Ceram. Soc.* **2009**, *29*, 1789–1794. [CrossRef]
17. Izoulet, A.; Guillemet-Fritsch, S.; Estournès, C.; Morel, J. Microstructure control to reduce leakage current of medium and high voltage ceramic varistors based on doped ZnO. *J. Eur. Ceram. Soc.* **2014**, *34*, 3707–3714. [CrossRef]
18. Onreabroy, W.; Sirikulrat, N.; Brown, A.P.; Hammond, C.; Milne, S.J. Properties and intergranular phase analysis of a ZnO–CoO–Bi_2O_3 varistor. *Solid State Ion.* **2006**, *177*, 411–420. [CrossRef]
19. Bai, S.; Tseng, T. Influence of sintering temperature on electrical properties of ZnO varistors. *J. Appl. Phys.* **1993**, *74*, 695–703. [CrossRef]
20. Zhang, C.; Xing, H.; Li, P.; Li, C.; Lv, D.; Yang, S. An Experimental Study of the Failure Mode of ZnO Varistors Under Multiple Lightning Strokes. *Electronics* **2019**, *8*, 172. [CrossRef]
21. Litzbarski, L.S.; Olesz, M.; Wojtas, S.; Winiarski, M.J.; Klimczuk, T.; Głowiński, H.; Andrzejewski, B. Quality Assessment of Low Voltage Surge Arresters. *IEEE Access* **2022**, *10*, 129313–129321. [CrossRef]
22. Das, A.K.; Dalai, S. Recent Development in Condition Monitoring Methodologies of MOSA Employing Leakage Current Signal: A Review. *IEEE Sens. J.* **2021**, *21*, 14559–14568. [CrossRef]
23. Munir, A.; Abdul-Malek, Z.; Arshad, R.N. Resistive Leakage Current Based Condition Assessment of Zinc Oxide Surge Arrester: A Review. In Proceedings of the 2021 IEEE International Conference on the Properties and Applications of Dielectric Materials (ICPADM), Johor Bahru, Malaysia, 12–14 July 2021; pp. 183–186.
24. Lira, G.; Costa, E. MOSA Monitoring Technique Based on Analysis of Total Leakage Current. *Power Deliv. IEEE Trans.* **2013**, *28*, 1057–1062. [CrossRef]
25. Khodsuz, M.; Mirzaie, M. Evaluation of ultraviolet ageing, pollution and varistor degradation effects on harmonic contents of surge arrester leakage current. *IET Sci. Meas. Technol.* **2015**, *9*, 979–986. [CrossRef]
26. Metwally, I.A.; Eladawy, M.; Feilat, E.A. Online condition monitoring of surge arresters based on third-harmonic analysis of leakage current. *IEEE Trans. Dielectr. Electr. Insul.* **2017**, *24*, 2274–2281. [CrossRef]
27. Das, A.K.; Ghosh, B.; Dalai, S.; Chatterjee, B. Sensing Surface Contamination of Metal Oxide Surge Arrester through Resistive Leakage Current Signal Analysis by Mathematical Morphology. *IEEE Sens. J.* **2020**, *20*, 9460–9468. [CrossRef]
28. Das, A.K.; Dalai, S.; Chatterjee, B. Deep learning–based surface contamination severity prediction of metal oxide surge arrester in power system. *IET Sci. Meas. Technol.* **2021**, *15*, 376–384. [CrossRef]
29. Fu, Z.; Wang, J.; Bretas, A.; Ou, Y.; Zhou, G. Measurement Method for Resistive Current Components of Metal Oxide Surge Arrester in Service. *IEEE Trans. Power Deliv.* **2017**, *33*, 2246–2253. [CrossRef]
30. Arshad, S.M.; Rodrigo, A.S. Modified Phase Shifting of Leakage Current to Condition Monitoring of Metal Oxide Surge Arresters in Power System. In Proceedings of the 2018 Moratuwa Engineering Research Conference (MERCon), Moratuwa, Sri Lanka, 30 May–1 June 2018; pp. 300–305.
31. Dobrić, G.; Stojanović, Z.; Stojković, Z. The application of genetic algorithm in diagnostics of metal-oxide surge arrester. *Electr. Power Syst. Res.* **2015**, *119*, 76–82. [CrossRef]
32. Schei, A. Diagnostics techniques for surge arresters with main reference to on-line measurement of resistive leakage current of metal-oxide arresters. In *Proceedings of the International Conference on Large High Voltage Electric Systems (CIGRÉ 2000)*; International Conference on Large High Voltage Electric Systems: Paris, France, 2000; pp. 1–10.
33. Shirakawa, S.; Endo, F.; Kitajima, H.; Kobayashi, S.; Goto, K.; Sakai, M. Maintenance of surge arrester by a portable arrester leakage current detector. *IEEE Trans. Power Deliv.* **1988**, *3*, 998–1003. [CrossRef]
34. Khavari, A.H.; Munir, A.; Abdul-Malek, Z. Circuit-based method for extracting the resistive leakage current of metal oxide surge arrester. *Bull. Electr. Eng. Inform.* **2020**, *9*, 2213–2221. [CrossRef]
35. Lundquist, J.; Stenstrom, L.; Schei, A.; Hansen, B. New method for measurement of the resistive leakage currents of metal-oxide surge arresters in service. *IEEE Trans. Power Deliv.* **1990**, *5*, 1811–1822. [CrossRef]

36. Abdul-Malek, Z.; Novizon, A. A new method to extract the resistive component of the metal oxide surge arrester leakage current. In Proceedings of the 2008 IEEE 2nd International Power and Energy Conference, Johor Bahru, Malaysia, 1–3 December 2008; pp. 399–402.
37. Khodsuz, M.; Mirzaie, M. An improved time-delay addition method for MOSA resistive leakage current extraction under applied harmonic voltage. *Measurement* **2016**, *77*, 327–334. [CrossRef]
38. Han, Y.; Li, Z.; Zheng, H. A new method to extract the resistive current of MOA based on least square. In Proceedings of the 2015 IEEE 11th International Conference on the Properties and Applications of Dielectric Materials (ICPADM), Sydney, NSW, Australia, 19–22 July 2015; pp. 312–315.
39. Han, Y.; Li, Z.; Zheng, H.; Guo, W. A Decomposition Method for the Total Leakage Current of MOA Based on Multiple Linear Regression. *IEEE Trans. Power Deliv.* **2016**, *31*, 1422–1428. [CrossRef]
40. Das, A.K.; Chatterjee, S.; Chatterjee, B.; Dalai, S. Cross Spectrum Aided Surface Condition Assessment of Metal Oxide Surge Arrester Employing Convolutional Neural Network. *IEEE Trans. Dielectr. Electr. Insul.* **2021**, *28*, 2134–2143. [CrossRef]
41. *IEC 60507:2013*; Artificial Pollution Tests on High-Voltage Ceramic and Glass Insulators to Be Used on a.c. Systems. International Electrotechnical Commission: Geneve, Switzerland, 2013.
42. Barbosa, V.R.N.; Lira, G.R.S.; Dias, M.B.B.; Costa, E.G. Estimation of Metal Oxide Surge Arresters' Useful Life Based on Time Series Forecasts. *IEEE Trans. Power Deliv.* **2022**, *37*, 842–850. [CrossRef]
43. Instytut Energetyki. Urządzenie Do Diagnozowania Stanu Zużycia Ograniczników Przepięć, Zwłaszcza Ograniczników Znajdujących Się W Eksploatacji. PL Patent 194370 B1, 23 January 2001.
44. Olesz, M. Determining the leakage current resistive component by the orthogonal vector method. In Proceedings of the 2018 34th International Conference on Lightning Protection (ICLP), Rzeszow, Poland, 2–7 September 2018; pp. 1–4.
45. *EN 50160:2010*; Voltage Characteristics of Electricity Supplied by Public Electricity Networks 2010. International Electrotechnical Commission: Geneve, Switzerland, 2010.
46. *EN 61869-1:2009*; Instrument Transformers—Part 1: General Requirements. International Electrotechnical Commission: Geneve, Switzerland.
47. *EN 61869-3:2011*; Instrument Transformers—Part 3: Additional Requirements for Inductive Voltage Transformers. International Electrotechnical Commission: Geneve, Switzerland.
48. Hinrichsen, V. *Metal-Oxide Surge Arresters in High-Voltage Power Systems*; Siemens: Munich, Germany, 2001; Volume 1.
49. Larsen, V.; Lien, K. In-service testing and diagnosis of gapless metal oxide surge arresters. In Proceedings of the Materiały IX International Symposium on Lightning Protection, Foz do Iguaçu, Brazil, 26–30 November 2007.
50. Li, S.; Xie, F.; Liu, F.; Li, J.; Alim, M.A. The relation between residual voltage ratio and microstructural parameters of ZnO varistors. *Mater. Lett.* **2005**, *59*, 302–307. [CrossRef]
51. Sawalha, A.; Abu-Abdeen, M.; Sedky, A. Electrical conductivity study in pure and doped ZnO ceramic system. *Phys. B Condens. Matter* **2009**, *404*, 1316–1320. [CrossRef]
52. EPCOS AG. *General Technical Information*; SIOV Met. Oxide Varistors; EPCOS AG: Munich, Germany, 2011.
53. Fernández-Hevia, D.; de Frutos, J.; Caballero, A.C.; Fernández, J.F. Bulk-grain resistivity and positive temperature coefficient of ZnO-based varistors. *Appl. Phys. Lett.* **2003**, *82*, 212–214. [CrossRef]
54. Olesz, M. Algorytmy obliczania składowej czynnej prądu upływu ograniczników przepięć. *Przegląd Elektrotechniczny* **2012**, *88*, 30–33.
55. Fujiwara, Y.; Shibuya, Y.; Imataki, M.; Nitta, T. Evaluation of Surge Degradation of Metal Oxide Surge Arrester. *IEEE Trans. Power Appar. Syst.* **1982**, *PAS-101*, 978–985. [CrossRef]
56. Wooi, C.; Abdul-Malek, Z.; Mashak, S.V. Effect of ambient temperature on leakage current of gapless metal oxide surge arrester. *J. Teknol.* **2013**, *64*, 157–161. [CrossRef]
57. Xu, Z.; Zhao, L.; Ding, A.; Lu, F. A Current Orthogonality Method to Extract Resistive Leakage Current of MOSA. *IEEE Trans. Power Deliv.* **2013**, *28*, 93–101. [CrossRef]
58. Fernando, S.N.; Raghuveer, M.R. Technique to examine the influence of voltage harmonics on leakage current based MOSA diagnostic indicator. In Proceedings of the 2000 Annual Report Conference on Electrical Insulation and Dielectric Phenomena (Cat. No. 00CH37132), Victoria, BC, Canada, 15–18 October 2000; Volume 2, pp. 596–599.